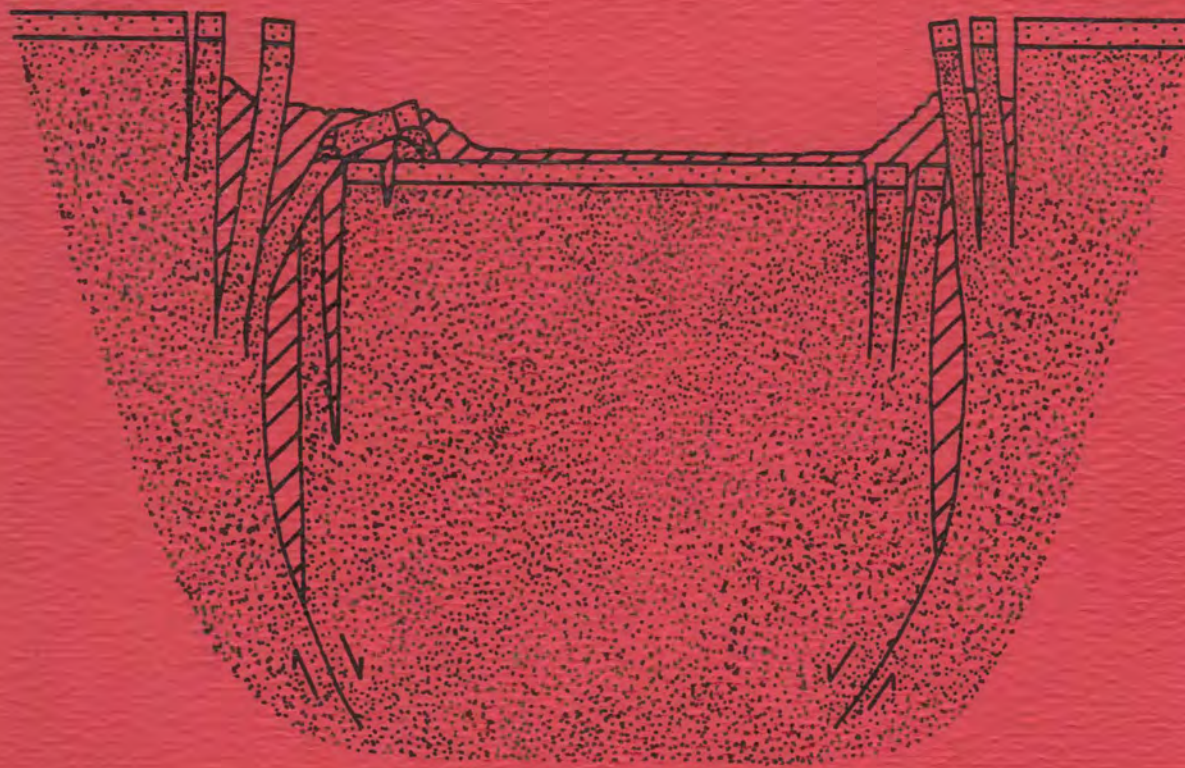


A MODEL FOR GRABEN  
FORMATION BY SUBSURFACE FLOW;  
CANYONLANDS NATIONAL PARK, UTAH

BY

GEORGE E. MCGILL

ALBERT W. STROMQUIST



CONTRIBUTION NO. 15  
DEPARTMENT OF GEOLOGY AND GEOGRAPHY  
UNIVERSITY OF MASSACHUSETTS  
AMHERST, MASSACHUSETTS

A MODEL FOR GRABEN FORMATION BY  
SUBSURFACE FLOW; CANYONLANDS NATIONAL PARK, UTAH.

by

George E. McGill  
Albert W. Stromquist

Contribution No. 15  
Department of Geology and Geography  
University of Massachusetts  
Amherst, Massachusetts

June, 1974



## TABLE OF CONTENTS

	Page
ABSTRACT . . . . .	1
INTRODUCTION . . . . .	4
THE CANYONLANDS GRABEN . . . . .	7
General Setting . . . . .	7
Mechanical Model for Formation of Canyonlands Graben . . . . .	8
Geometry of Canyonlands Graben. . . . .	16
Validity of Baker Model . . . . .	32
EXPERIMENTAL SIMULATION. . . . .	44
Introduction. . . . .	44
Experimental Results. . . . .	48
Conclusions from Model Studies. . . . .	50
THEORETICAL ANALYSIS . . . . .	52
The Glacier Flow Model. . . . .	52
Application of Glacier Model to Scale-model Experiments. . . . .	58
Validity of Glacier Model for Canyonlands Graben . . . . .	68
DISCUSSION AND CONCLUSIONS . . . . .	70
REFERENCES . . . . .	78

## ILLUSTRATIONS

Figure	Page
1. Location of Canyonlands Graben . . . . .	9
2. Canyonlands Graben Complex . . . . .	11
3. Index to Topographic Features. . . . .	13
4. Aerial Oblique View of Graben Complex. . . . .	15
5. Aerial Oblique View of Northwest-trending Fracture Zone . . . . .	15
6. Detail of Jointing . . . . .	17
7. Idealized Pre-faulting Cross Section of Graben Region . . . . .	19
8. Possible Fault Responses to Stresses Superposed by Subsurface Flow . . . . .	21
9. North End of Devils Lane Graben. . . . .	23
10. En Echelon Offset Near North End of Devils Lane Graben . . . . .	23
11. Aerial Detail of Faults, North End of Devils Lane Graben. . . . .	25
12. Ground Close-up of Faulted Slabs, North End of Devils Lane Graben . . . . .	25
13. Septum near South End of Devils Lane Graben. . . . .	27
14. South-facing Ramp at Devils Lane Septum. . . . .	27
15. North-facing Ramp at Devils Lane Septum. . . . .	29
16. Secondary Structures along Graben Walls, Canyonlands National Park . . . . .	31
17. Secondary Structures Expectable Along Walls of Graben with Curved, Inward-dipping Faults. . . . .	33
18. Dropped and Rotated Segment of Graben Wall, Red Lake Canyon . . . . .	35
19. Dropped and Rotated Segment of Graben Wall, Red Lake Canyon . . . . .	35

Figure	Page
20. Elongate Swallow Hole . . . . .	37
21. Crater-like Swallow Hole. . . . .	37
22. Sawtooth Nature of Graben Wall, Northern End Red Lake Canyon. . . . .	39
23. Sawtooth Nature of Graben Wall, Northern End Cyclone Canyon . . . . .	39
24. East Flank of Meander Anticline . . . . .	41
25. West Flank of Meander Anticline . . . . .	41
26. Anticline Trending Parallel to Lower Red Lake Canyon . . . . .	43
27. Pre- and Post-faulting Drainage Patterns. . . . .	45
28. Changes in Drainage Due to Graben Faulting. . . . .	47
29. Knick Point in Pre-faulting Stream Channel. . . . .	49
30. Small Anticline Confined to Pre-faulting Stream Channel. . . . .	51
31. Apparatus Used for Scale-model Experiments. . . . .	53
32. Experiment 2 Prior to Test. . . . .	55
33. Experiment 2 After 1 Hour and 56 Minutes (Oblique View) . . . . .	55
34. Experiment 2 After 1 Hour and 56 Minutes (Vertical View). . . . .	57
35. Experiment 2 After 2 Hours and 9 Minutes. . . . .	57
36. Experiment 2 After 3 Hours and 15 Minutes . . . . .	59
37. Experiment 4 Prior to Test. . . . .	61
38. Experiment 4 After 50 Minutes . . . . .	61
39. Experiment 4 After 2 Hours and 11 Minutes . . . . .	63
40. Experiment 4 After 3 Hours and 53 Minutes (Oblique View) . . . . .	63
41. Experiment 4 After 3 Hours and 53 Minutes (Vertical View). . . . .	65

Figure	Page
42. Flow Deformation of Paraffin . . . . .	65
43. Stress Model for Valley Glacier Applied to Model Experiments . . . . .	67
44. Principal Stresses at Two Levels in Model. . . . .	67
45. Mid-Atlantic Rift Fractures at Þingvellir, Iceland . . . . .	71
46. Mid-Atlantic Rift Fractures at Þingvellir, Iceland . . . . .	73
47. Mid-Atlantic Rift Fractures at Þingvellir, Iceland . . . . .	73
48. Graben in Tharsis Region of Mars . . . . .	77
49. Graben near Tharsis Region of Mars . . . . .	77

## ABSTRACT

Pleistocene/Recent canyon cutting by the Colorado River has exposed evaporites of the Paradox Member of the Hermosa Formation (Pennsylvanian) in Canyonlands National Park, Utah. Subsurface lateral flow of these evaporites into the Colorado River canyon (Cataract Canyon) has occurred due to stresses generated by unloading of the Paradox Member under the river. Thicknesses of rock overlying the Paradox Member range from 0 in the river canyon to almost 450m on valley divides immediately adjacent to the canyon and for many kilometers east and west of the canyon. Flow has been particularly active on the east side of the river because of the gentle regional dip to the west, toward the river canyon. This lateral flow in a subsurface layer has superposed essentially horizontal tensile stresses on the regional compressive stresses due to gravity. A series of distinctive structural features has developed in the brittle rocks overlying the Paradox Member in response to the evaporite flow and superposed stresses:

1. A pervasive, nearly rectilinear system of unusually wide open joints. The fracture anisotropy controlling the orientations of these joints is probably inherited from an earlier, unknown regional stress system.

2. A system of curved graben, concave towards the Colorado River (westward). The faults bounding these graben are vertical or nearly so in the open-jointed, near-surface rocks, but apparently dip inward toward graben axes in the rocks

immediately above the Paradox Member. Many complex fault features that might be considered evidence for multiple deformation may be readily understood as due to interaction between graben faults and pre-existing joints.

3. Broad, gentle anticlines trending parallel to the Colorado River and to the lower reaches of the major tributaries in the Canyonlands. These are due to upward flow of evaporites toward the erosion-created free surfaces. The trends of these anticlines follow the meanders of the valleys, and are thus genetically tied to drainage development. Domical plugs of evaporites tend to occur where major tributaries enter the Colorado River.

Scale-model simulations of the geometrical and mechanical features involved in the origin of the Canyonlands graben show similar structures, including graben faults that have interacted with early-formed joints. Mathematical models developed by Nye (1951, 1952, 1957, 1965) for valley glaciers are applicable to the scale models and, by extrapolation, to the Canyonlands graben complex. Fractures predicted for the brittle surface layers of valley glaciers are similar in pattern and type to those found in the scale models and in the field.

Graben (rille) complexes on Mars and the moon may be due to crustal extension due to arching, or to lateral flow beneath the surface. The Canyonlands graben are ideal analogues for graben formed by subsurface flow because they are so young and fresh that structural details normally lost by erosion are still present. Because of the relative slowness of erosion on

Mars and the moon, such details are likely preserved there, permitting us to use detailed geometrical arguments in our efforts to understand the mechanisms responsible for lunar and martian graben complexes.

## INTRODUCTION

This is a progress report on some of the research in planetary structural geology underway at the University of Massachusetts. Specifically, this report deals with field, experimental, and theoretical studies of the origin of young graben in Canyonlands National Park, Utah. These graben serve as analogues for straight and arcuate rilles on Mars and the moon. Most of the material presented is descriptive, and much of it is in the form of photographs. A possible theoretical model is outlined briefly; more complete development is left to further research, and to journal publication. As the reader will discover, much work of all types remains to be done.

Linear and arcuate rilles are common features on both the moon and Mars. These are interpreted to be graben by most workers. A graben is defined as a long, narrow down-thrown block formed by predominantly dip-slip movement on vertical or inward-dipping normal faults. On the moon and Mars, however, graben can be recognized only by their topographic expression, and can be studied only through analysis of their topographic characteristics and chronological relationships.

Simply calling straight and arcuate rilles "graben" tells us little except that the maximum compressive stress was approximately vertical and the intermediate and least compressive stresses were approximately horizontal during faulting (Anderson, 1951, p. 12). More precise designations of the orientations of principal stresses require some knowledge of

the degree and type of anisotropy of the stressed materials prior to faulting. Thus fracture analysis is critically dependent on accurate delineation of fracture chronology.

Even if we uniquely specify the orientations of the principal stresses during faulting, this knowledge only permits us to eliminate incompatible dynamic hypotheses for the origin of the graben-forming stresses. Stress orientations, by themselves, are incapable of uniquely determining the causative dynamic mechanism.

A number of dynamic mechanisms for the formation of large graben might be envisaged; three are of potential interest with regard to large-scale lunar and martian rilles. First, graben may form parallel to the axis of a large arch, due to the superposition of local tensile stresses caused by flexure on to the general regional stress field. Second, graben may form over regions of lateral spreading of the lithosphere as a result of deep-seated mantle processes causing plate motions. Third, graben may form in brittle surface layers if an underlying layer is capable of flow and the specific geometric or topographic conditions of the locality permit flow.

The first two of these three have been suggested as possible causes of the graben complex in the Tharsis region of Mars (Phillips, et al., 1973, p. 4819; Hartmann, 1973, p. 4102). Quaide (1965) explains rilles concentric to Mare Humorum with a mechanism similar to the first of these. There is a strong possibility that permafrost layers exist on Mars (Sharp, et al., 1971; Sagan, et al., 1973). If so, one could

envisage these being melted from below by geothermal heat in a volcanic region such as Tharsis, yielding the requisite brittle over "viscous" layering for the operation of the third of the suggested mechanisms.

In the foreseeable future, the only way to decide which, if any, of these mechanisms is active on another planet is to look for diagnostic features in the structures visible on photographs. Are there any characteristics of the geometry or the chronology of graben that permit a choice among these possibilities? Our studies are directed ultimately at the answer to this question.

This study has been supported by NASA grants NGR-22-010-076 from the Office of Planetary Programs, and NGR-22-010-052 from the Apollo Lunar Exploration Office. The manuscript was critically reviewed by L. M. Hall and D. U. Wise. Figures were drafted by J. K. Lucey. The Astrogeology Branch, U. S. Geological Survey, Flagstaff provided a vehicle and equipment for the field work in Canyonlands National Park. The Office of Planetary Programs, NASA, and Edward J. Zeller, University of Kansas, provided the aircraft needed for the aerial photographs. Chris Condit of the U.S.G.S. and Edward Zeller of the University of Kansas contributed materially to the success of the aerial photography by their skillful piloting.

## THE CANYONLANDS GRABEN

General Setting

A complex of very young graben occurs east of the Colorado River in Canyonlands National Park, Utah, extending from the confluence of the Green and Colorado Rivers southwestward about 25Km (Figs. 1 and 2). Individual graben have vertical walls and flat floors. Topographic relief is up to about 100m with an average graben depth of 30 to 50m. The graben are up to 8Km long, and range from 0 to 400m wide, with a typical value for graben width of 150 to 200m. Most of the graben are from 700 to 1000m apart.

The graben complex is divided into a northern portion characterized by a spectacular, nearly rectilinear grid of vertical joints (Figs. 4 and 6), and a southern portion with much more subdued jointing, the dividing line occurring along a well defined northwest-trending fracture zone (Figs. 2 and 5). The joints appear to be older than the graben faults, for reasons which will be developed in a later section of this report. Most of our work has been in the northern part of the graben complex, for which an index is provided (Fig. 3).

Throughout most of the graben area, the surface rock is the Cedar Mesa Formation of the Cutler Group. Isolated spires and walls of the Organ Rock Tongue of the Cutler Group stand above this surface at many places. Graben and cross canyons expose the Rico Formation and the upper part of the Hermosa Formation. Along the banks of the Colorado River and

for short distances up the deepest side canyons, the upper part of the Paradox Member of the Hermosa Formation is also exposed. All of these rocks are Pennsylvanian or Permian (Lewis and Campbell, 1965). Baars (1962) has published a thorough description of the Permian rocks of the Colorado Plateau. Lewis and Campbell (1965) discuss the stratigraphic section of the Canyonlands area, and have published a small-scale geologic map of a sizeable portion of southeastern Utah, including most of the Canyonlands graben complex. Stratigraphic terminology used in this report is that of Lewis and Campbell (1965).

#### Mechanical Model for Formation of Canyonlands Graben

Baker (1933, p. 74) suggested that the Canyonlands graben resulted from flow of gypsum in the Paradox Member down the gentle regional westward dip into the Colorado River. Lewis and Campbell (1965, p. B31) demonstrated that the gypsum of the Paradox Formation is exposed along the Colorado Canyon for a distance almost exactly coinciding with the arcuate graben complex. Rocks of the Hermosa, Rico and Cedar Mesa Formations are arched into an anticline which follows the meanderings of the Colorado River, and which was termed the "Meander Anticline" by Harrison (1927, p. 123-127). Harrison postulated that the anticline was caused by upward flow of evaporites as the load on the Paradox Formation was relieved by downcutting of the Colorado River.

If Baker's hypothesis is correct, the Canyonlands graben

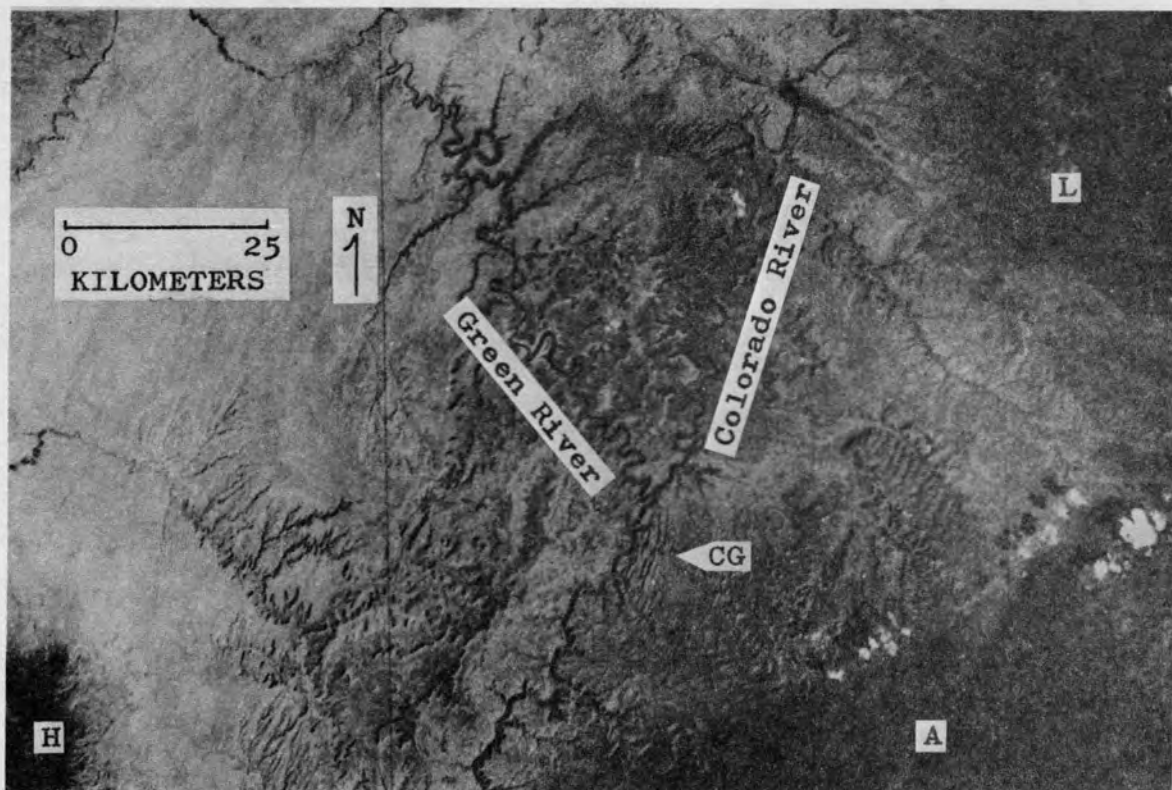


Figure 1: Location of Canyonlands graben. CG = Canyonlands graben; A = Abajo Mountains; H = Henry Mountains; L = LaSalle Mountains. Scale of this photograph is roughly comparable to scale of most Mariner 9 B-frames, indicating order-of-magnitude size difference between Canyonlands graben and most Tharsis Ridge graben. NASA ERTS-A photograph.

-----

represent a well exposed and very young example of graben formed by lateral flow of a "viscous" layer beneath brittle surface layers, the third of the three dynamic mechanisms mentioned in the introduction.

Some major questions to be asked in the field and in the laboratory relevant to the martian and lunar graben include:

1. What are the geometric and mechanical characteristics

of graben formed by the lateral flow mechanism?

2. Are there any distinctive features, identifiable remotely, that indicate this mechanism has occurred?
3. Are there geometric characteristics indicative of the depth to the flowing layer?
4. Is there any way to estimate the total amount of lateral extension?

In addition, we have tested the validity of the Baker hypothesis and, for purposes of experimentation, obtained some knowledge of the characteristic rate of the process. The bulk of this report deals with the verification of the mechanism, the age of the faulting, and the geometric and mechanical characteristics of the graben.

Figure 7 is an idealized WNW-ESE pre-faulting cross section, representative of all but the end regions of the graben complex, that illustrates the salient points of the Baker hypothesis. The lateral flow in the Paradox Member superposes a WNW-ESE tension onto the general compressive stresses due to gravity, which would yield principal stress orientations such that  $\sigma_1$  (compressive stresses positive) would be approximately vertical,  $\sigma_3$  would be approximately parallel to the bedding and oriented in the direction of the regional dip (normal to Cataract Canyon), and  $\sigma_2$  would be parallel to the strike of the bedding and thus to the long dimension of the total complex of graben. Throughout most of the stressed rock, all stresses would remain compressive, though close to the surface a tensile  $\sigma_3$  is likely.



Figure 2: Canyonlands graben complex. FZ = northwest-trending fracture zone along Chesler Canyon dividing highly jointed northern portion of graben complex from less spectacularly jointed southern portion. See Fig. 3 for identification of graben discussed in text. U. S. Geological Survey photomosaic.

Figure 8 illustrates some possible fault responses to such a stress field, all of which would produce graben. Field evidence favors the model illustrated by Fig. 8d. Moreover, this model is consistent with the results of laboratory experiments investigating the orientation of brittle fractures in rock samples tested at different confining pressures (e.g., Griggs and Handin, 1960). The geometry illustrated in Fig. 8d is thus explainable by basic rock mechanics alone. However, the near-surface rocks in the area now occupied by the graben were broken by a pervasive grid of vertical joints (Fig. 6) prior to graben faulting, one set of which is roughly parallel to the trend of the graben. Consequently, we believe that these joints are responsible for the vertical dips of the faults near the surface, though the confining pressure, joints, and the mechanical properties of the various rock types together would determine the depth at which fault attitudes change from vertical to inclined.

If asked to sketch a cross section of a graben, most geologists would draw something similar to Fig. 8b. This is mechanically the most reasonable model on a planet where rapid erosion will have removed the uppermost levels of most graben, the only place where vertical faults are mechanically predictable. Presumably, we see the near-surface vertical faulting at Canyonlands only because the faults are very young and the graben essentially uneroded. On planets where erosion proceeds at rates orders of magnitude less than on earth, the most reasonable model for the attitudes of graben faults near

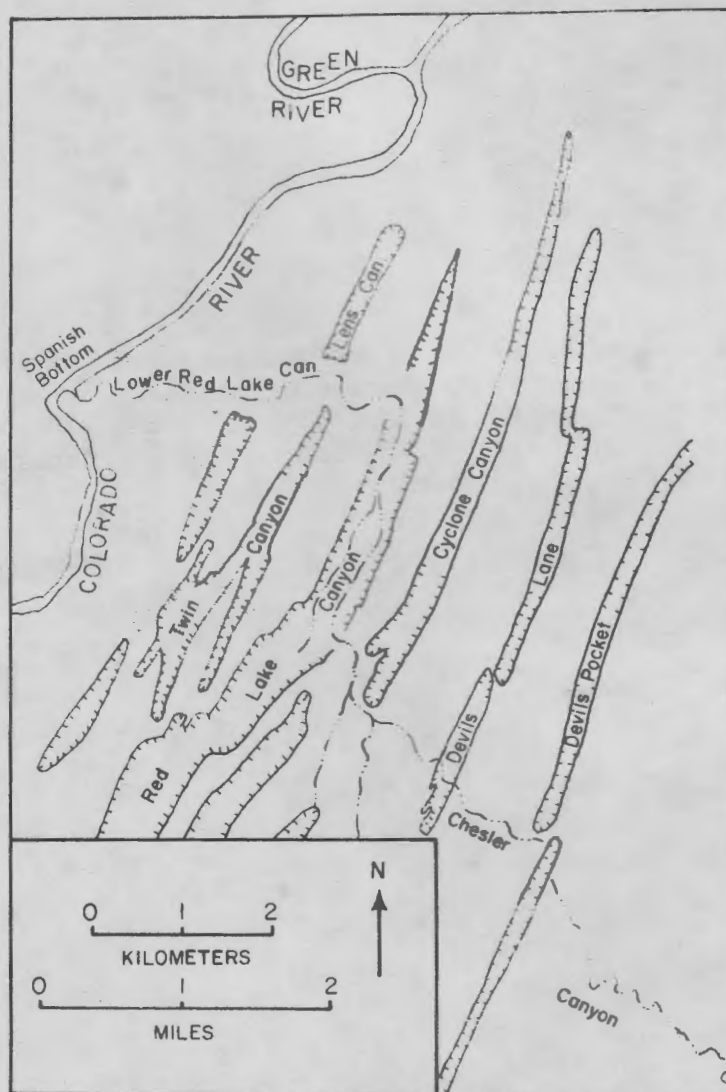


Figure 3: Index to topographic features in the northern part of the Canyonlands Graben complex. Features named are those illustrated and referred to in the text of this report.

the present surface is not obvious.

The model illustrated by Fig. 8a is mechanically unsound unless we postulate a very brittle, strong material overlain

Figure 4: Aerial oblique view of graben complex, looking south. Contrast between jointing of northern and southern portions clearly visible. DL = Devils Lane graben; CC = Cyclone Canyon graben; RLC = Red Lake Canyon graben.

Figure 5: Aerial oblique view of northwest-trending fracture zone along Chesler Canyon, looking northwest. Note extreme openness of joints along trend of fracture zone.



by a thin cover of weak, relatively non-cohesive materials. This is a poor model for the Canyonlands, but may well be a good one for many lunar rilles where an unconsolidated regolith overlies a brittle rock substrate. If the surface of Mars is underlain by varying thicknesses of fine-grained, poorly consolidated crater ejecta and aeolian deposits, this may be a valid model for some martian rilles also.

It is instructive to determine the lateral extension necessary to cause each of the four fault geometries considered (see Fig. 8). Clearly, we can determine very little about the amount of lateral extension from the vertical displacement of a graben unless we have some clue concerning the attitude of the bounding faults, both near the surface and at depth.

#### Geometry of Canyonlands Graben

The best evidence concerning the geometry and nature of movement along the faults occurs at the ends of graben where the slip is dying out, and on the septa between the overlapping segments of en echelon graben. Figures 9 through 15 illustrate the nature of this evidence and, with their captions, tell their own story. The overall impression is that of a giant deck of cards standing on edge, with individual cards or bundles of cards slipping downward varying distances. The exposures are so fresh and uneroded that the reality of the vertical or near-vertical slip on vertical faults is undeniable. The graben die out along rigidly rotated ramps at the ends, with or without cross faults (Figs. 13 through 15). Clearly,

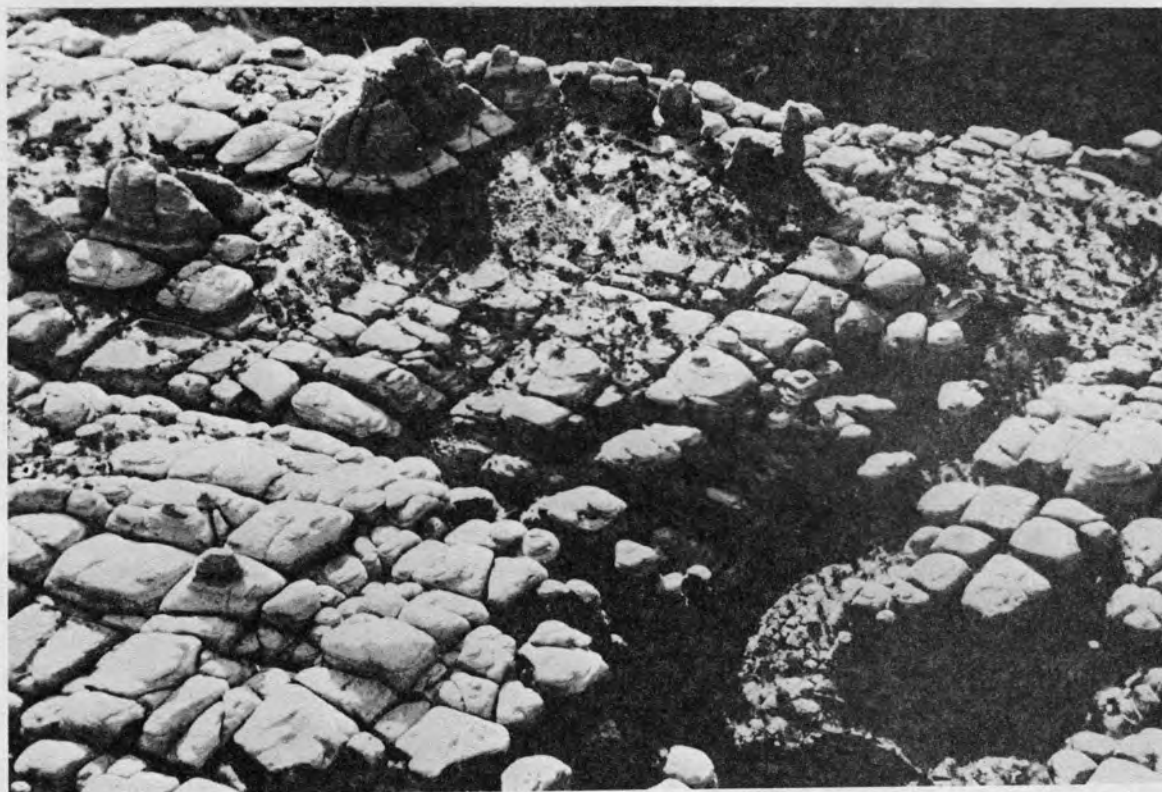


Figure 6: Detail of jointing in northern portion of graben complex. Joint blocks are typically 40m on a side. Joints in many places have been widened sufficiently by weathering to permit (require!) travel beneath the ground surface, at depths up to 20m.

-----

Fig. 8b does not represent a valid model for these graben.

One can connect bedding planes from one inter-graben divide to the next and reconstruct an essentially smooth, gently dipping surface (except close to Cataract Canyon, where the fault geometry is more complex). This implies that the absolute movement is downward in the graben, whereas the inter-graben divides simply moved laterally towards the Colorado

River. If the graben were formed by regional arching, or by differential vertical movement of rigid blocks "floating" on a gypsum layer, any initial, simple regional dip on the inter-graben divides could not survive. This absence of evidence for differential movement, combined with mechanical considerations and problems of volume displacement within the gypsum layer, suggests that Fig. 8c does not represent a valid model for the Canyonlands graben.

A study of Fig. 8d shows that movement on the faults shown must inevitably open huge cracks between the graben walls and floors, unless other processes act to fill these cracks. Figure 16 illustrates some of the secondary structures that have formed in the Canyonlands graben in response to movement on the faults bounding the graben. Any graben bounded by faults with dip angles decreasing with depth must adjust to excess space along the bounding faults near the surface. In the case of faults that are still dipping inward at the surface, the predicted geometry and sense of rotation is different than shown in Fig. 16. Figure 17 illustrates how a graben bounded by curved inward-dipping faults that extend to the surface might be modified by secondary structures so as to fill the incipient excess space.

Figures 18 and 19 illustrate secondary structures in the Canyonlands similar to some of those shown in Fig. 16. Because of alluvial and aeolian fill in the graben, very few exposures of downthrown blocks exist. However, the presence of crater-like depressions in the fill where both water and

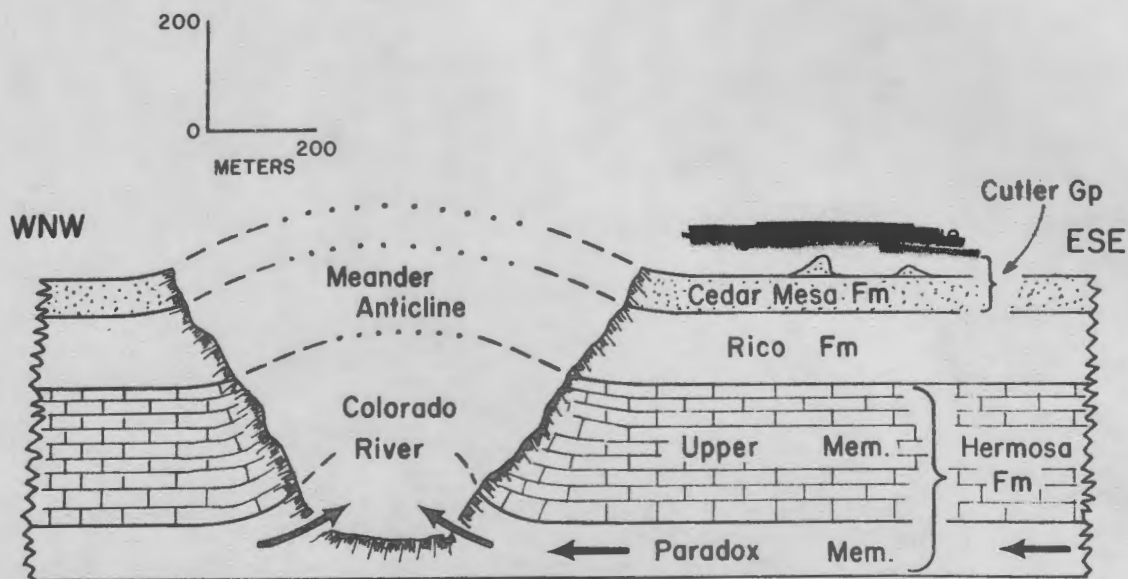
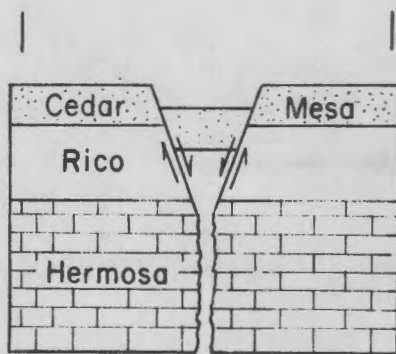


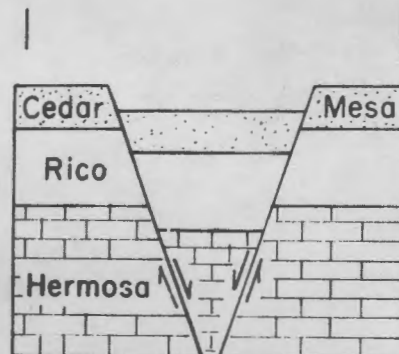
Figure 7: Idealized pre-faulting cross section of the graben region illustrating how canyon cutting by the Colorado River permitted lateral flow (arrows) of Paradox gypsum down the gentle westward regional dip and upward into Cataract Canyon. This flow superposed a WNW-ESE tensile stress onto the overall gravitational compressive stresses in the rocks above the Paradox, causing graben faulting (Fig. 8). The flow of the gypsum upward into Cataract Canyon and its deeper tributaries caused arching of the rocks overlying the Paradox, creating the Meander Anticline (Figs. 24 and 25) and other related folds (Fig. 26). As indicated by the western-most arrow, there has been some limited flow of gypsum into the river canyon from the western side of the river as well. Flow-related structures on the western (down-dip) side of the Colorado River are restricted to a narrow belt adjacent to the river (Fig. 25).

unconsolidated sediment have drained into the subsurface (Figs. 20 and 21), and the bridging of cracks by unconsolidated fill, analogous to snow bridges over glacier crevasses (Lewis and Campbell, 1965, p. B31) are at least consistent

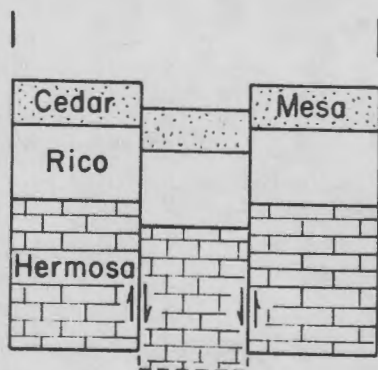
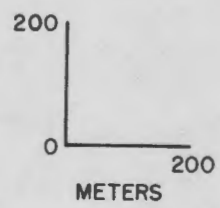
Figure 8: Some possible fault responses to the stresses superposed on the rocks by the flow cartooned in Fig. 7. Field observations of a most superficial nature are sufficient to eliminate models a and b from consideration for the Canyonlands graben. Model d is favored over model c because the overall geometry of faults in the area is more consistent with it (see text and supporting illustrations). Model a is attractive for weak or incoherent surface materials overlying strong, brittle rock, such as we find over much of the moon. Model b is the one considered "normal" by most geologists. The difference in width between the drawings and the small vertical lines above each drawing represents the lateral extension necessary to produce a graben of the width and vertical displacement shown. Even though all the graben are drawn with the same vertical displacement, this lateral extension differs among the models, pointing out the necessity of determining graben geometry in three dimensions in order to predict lateral extension from vertical displacement.



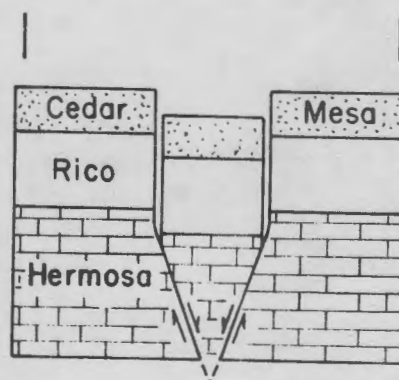
a



b



c



d

Figure 9: North end of Devils Lane graben, looking southwest. Faults are well exposed near center of picture where the graben segments are en echelon. Note line of pinnacles (~~Cedar Mesa sandstone~~) which is dropped into graben. Jointed surface is Cedar Mesa sandstone. Section of Park road known as the "Silver Stairs" (arrow) is located where road crosses line of ~~Cedar Mesa sandstone~~ pinnacles.

Figure 10: Closer view of en echelon offset of Devils Lane graben shown in Fig. 9, looking south. Northern segment of graben dies out because fault slips decrease southward. Elongate, down-dropped slabs of Cedar Mesa sandstone at terminus of graben are rigidly rotated along vertical faults which follow older joint planes. Note implication of scissors motion on fault(s) forming east (left) side of northern (closest) graben segment and west side of southern graben segment.

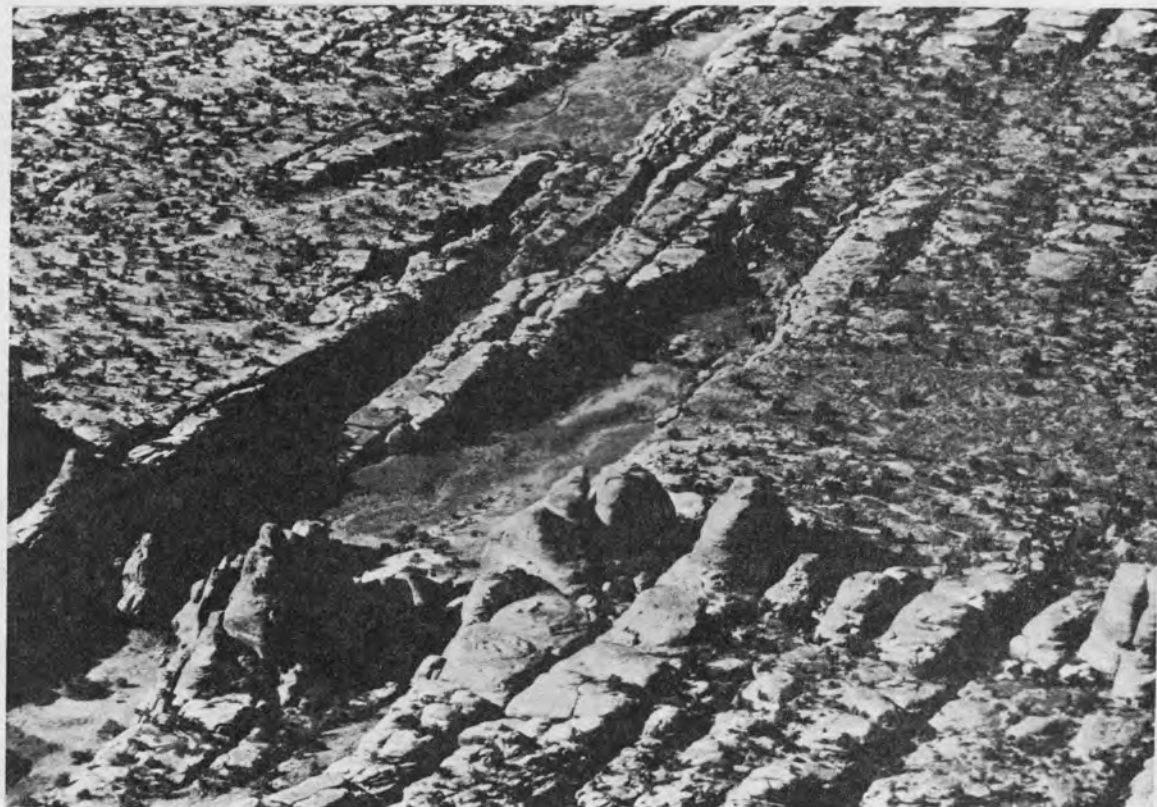
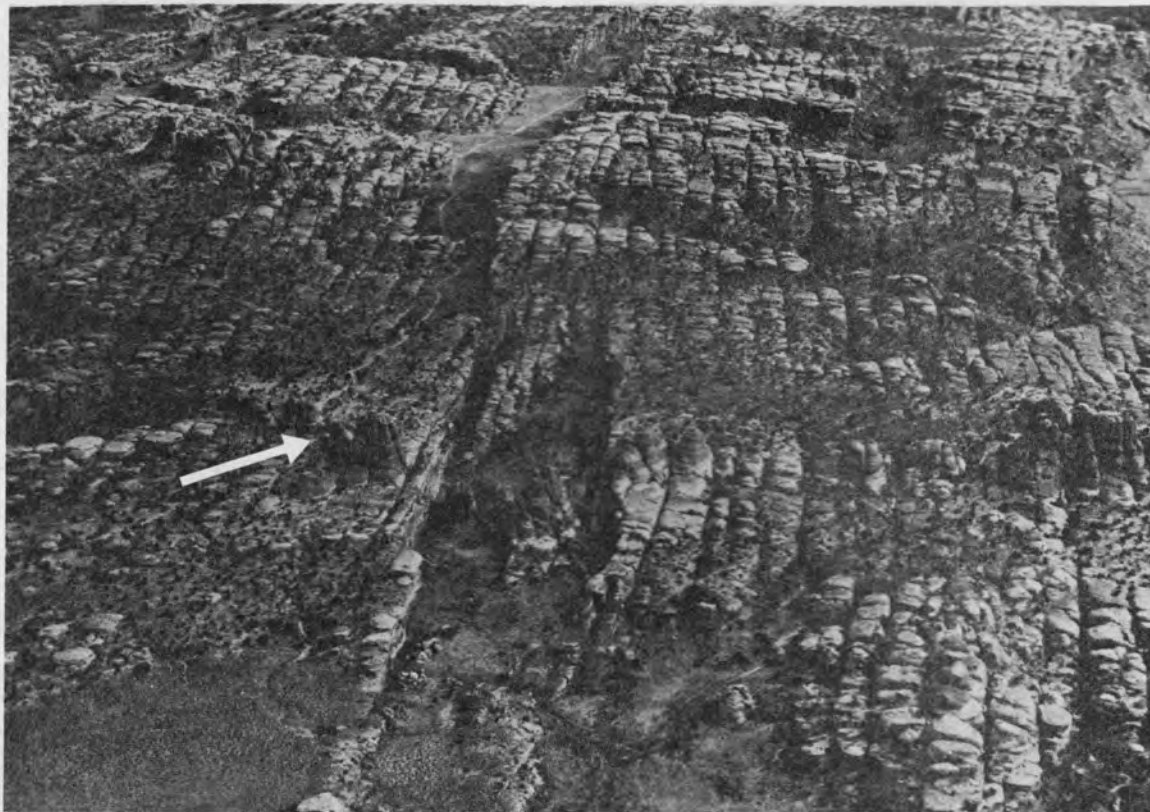


Figure 11: Detail of an echelon offset shown in Figs. 9 and 10, looking northeast. Differential vertical motion on different fault-bounded slabs of Cedar Mesa sandstone is apparent, even though total effect is that of a ramp forming the terminus of the graben segment. Necessity of vertical fault motions is particularly clear in this view. Arrow indicates approximate orientation of camera axis for Figure 12.

Figure 12: Side view of fault-bounded slabs in upper center of Fig. 11, looking east. Note simplicity of structure: there is no folding and no significant cross faulting. Rock is sandstone of Cedar Mesa Formation.

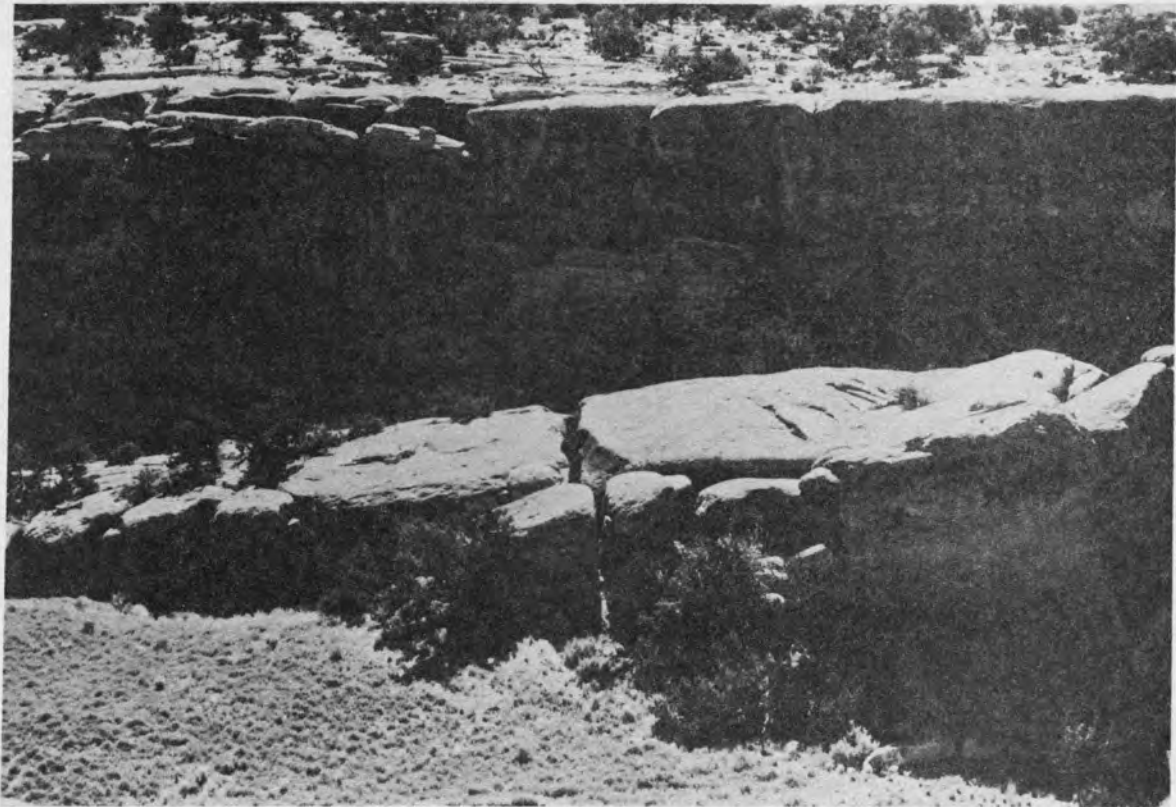
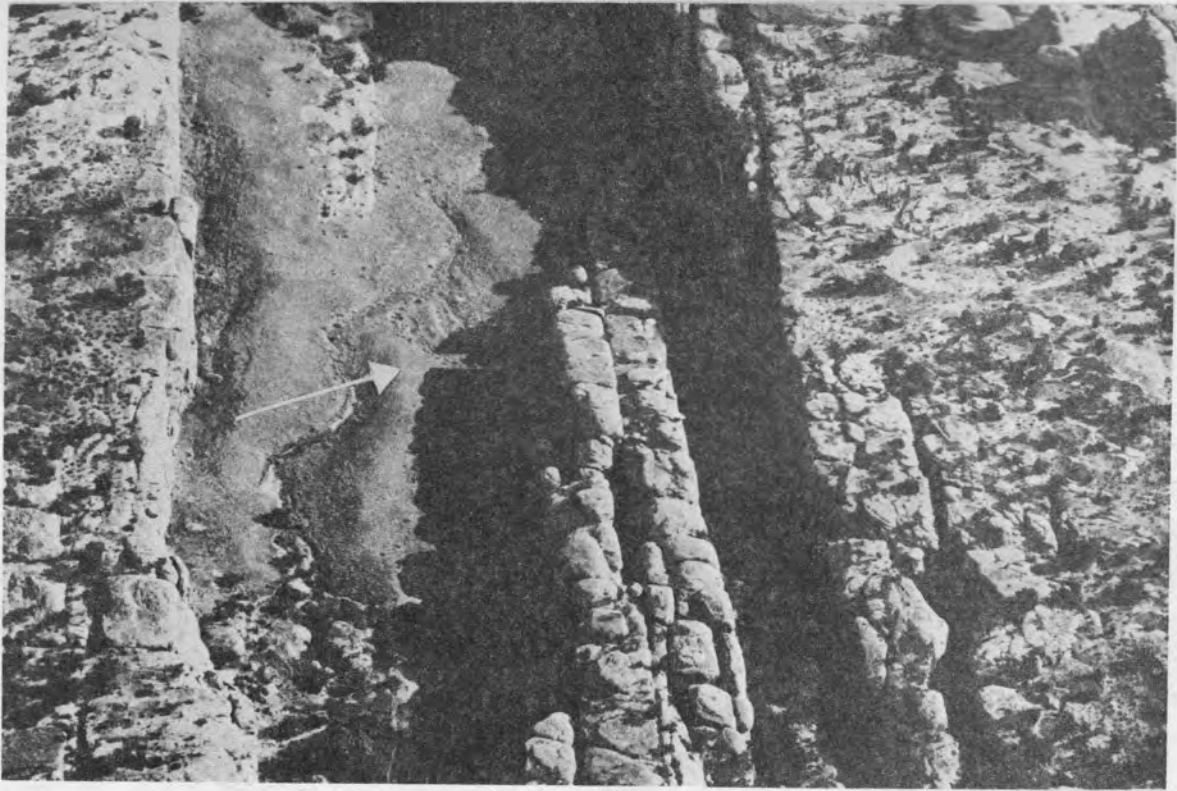
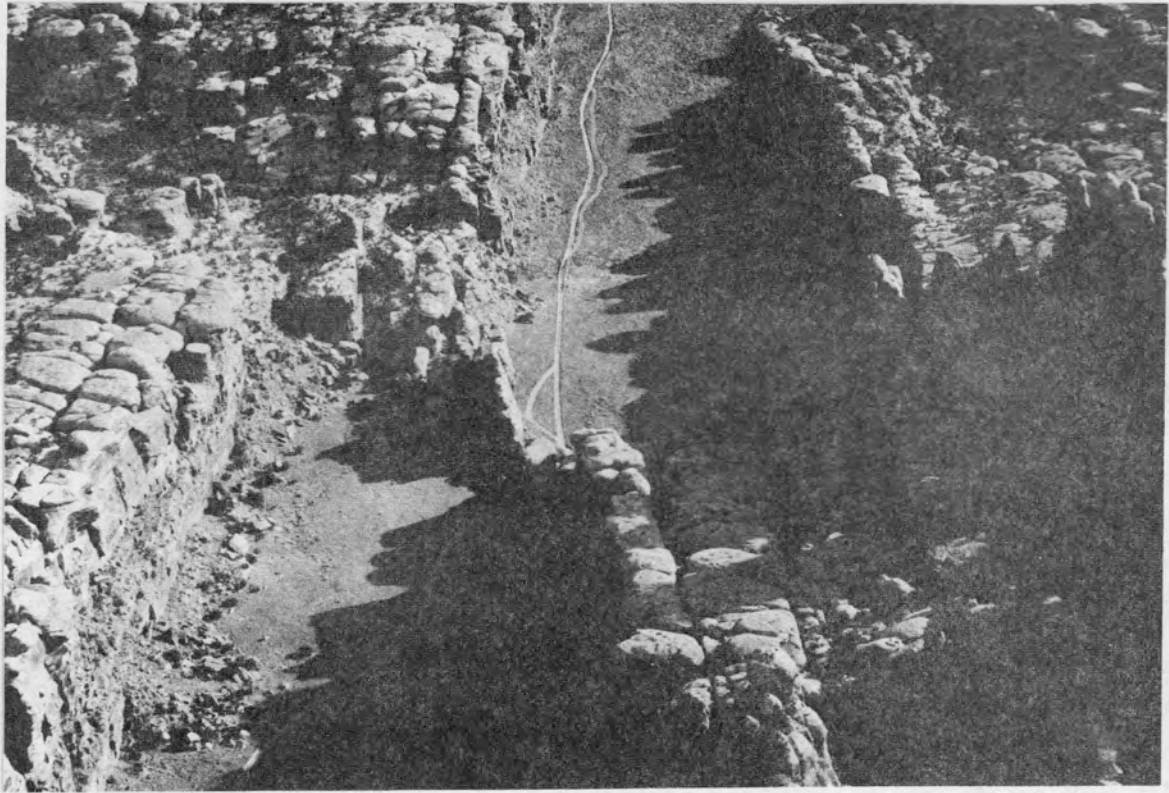


Figure 13: Septum near south end of Devils Lane graben, looking northeast. Both en echelon segments of the graben terminate in ramps. The septum is a narrow, tilted wall that is bounded on both sides by faults; thus it is an extremely thin horst. South facing ramp to left is illustrated in Fig. 14, north-facing ramp to right in Fig. 15. Fork in road on far side of septum leads to Indian paintings located on the septum.

Figure 14: South-facing ramp at Devils Lane septum. This is a simple ramp: there is no significant cross faulting, and only minor differential vertical motion on the fractures separating the southward tilted slabs of Cedar Mesa. The transverse vertical face at the left edge of the photograph is a cross fault with substantial slip (it is actually more clearly portrayed in Fig. 13). Note characteristic toadstool pedestals of jointed and weathered Cedar Mesa Formation.



with lateral movement and outward rotation within the down-thrown block.

As mentioned above, the entire area of the graben and much of the surrounding area was highly jointed prior to graben formation. For reasons that we do not understand, this jointing is unusually well developed in the northern portion of the graben complex. Although we believe that the joints predate the graben, we do not know if they formed immediately prior to faulting, or if they are much older. There is an interesting geometrical relationship between the joints and the graben. For much of their length, the graben walls roughly parallel one of the joint sets. In fact, it is this joint set that provides the fault planes near the surface (cf. Figs. 10 and 11). The other joint set is locally utilized for cross faulting, as on ramps (Fig. 15). These relationships tempt one to suggest that the joints directly controlled the orientation of the graben. However, near their northern terminations, where we have investigated this relationship, it is clear that the graben trend is not parallel to the jointing, even though the faults are old joint planes at almost all places where they are exposed. The result is a "sawtooth" effect along the graben walls (Figs. 22 and 23) in those places where the graben trend is not parallel to either set of older joints. This is consistent with the formation of non-vertical graben faults immediately above the Paradox Member, where the superposed tensile stress would be largest, and later propagation of these faults upward. In the near-surface rocks, these



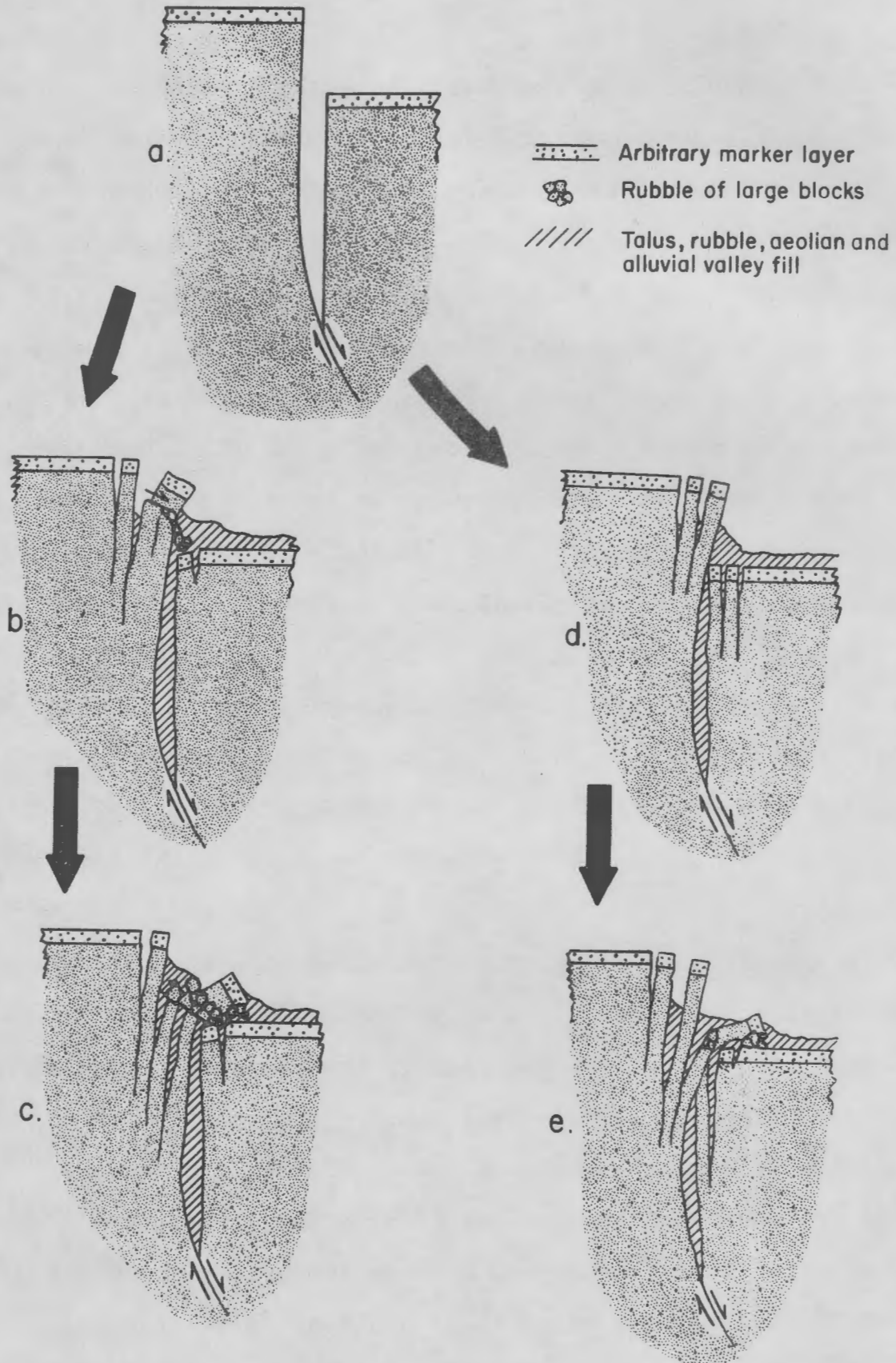
Figure 15: Looking south at north-facing ramp of Devils Lane septum. This is a more complex ramp than the south-facing one illustrated in Fig. 14. There is significant motion on both the fractures separating the northward tilted slabs and on the cross faults which segment these slabs. Note progressive widening of longitudinal faults and joints towards the camera due to rotation of narrow, unstable walls toward adjacent graben floor.

-----

upward-propagating faults were reoriented in detail in conformity with the older, vertical joints.

Figure 16: Secondary structures along graben walls in Canyonlands National Park. The vertical faults are interpreted to pass downward into faults dipping inward, producing incipient gaps between the upthrown and downthrown blocks of the graben (a). If the faults were single, this incipient space could be filled by rotation towards the fault of the entire downthrown block. In one case of a graben, this solution is not possible. In the Canyonlands graben, the space has been at least partly filled by inward rotation of joint-bounded slabs from the upthrown block, producing structures cartooned here. The sequences b to c and d to e may be observed along strike in the field. Two differences are illustrated by the b to c and d to e sequences:

1. Simple inward rotation of a joint-bounded slab (d to e) vs. rotation with detachment and sliding (b to c).
2. Rotation of thin slabs (d to e) vs. rotation of thick slabs (b to c). Simple rotation of thick slabs and detachment of thin slabs also have been observed.



### Validity of Baker Model

Evidence for the hypothesis that the graben were formed in brittle layers overlying laterally flowing evaporites of the Paradox Member is abundant, but primarily circumstantial. Figures 24 and 25 clearly illustrate that the gentle regional dip toward the Colorado River is reversed near the River, and that Harrison's "Meander Anticline" really exists. Furthermore, similar anticlines, dying upstream, exist in at least some of the deeper tributary canyons (Fig. 26). These anticlines faithfully follow the meander patterns of the valleys concerned. Because such a sinuous pattern is not normally characteristic of anticlinal axial surfaces, the inverse hypothesis -- that the valleys were eroded in fractured rock along the axial surfaces of pre-existing anticlines -- seems highly unlikely. Sheared gypsum, and dome-like folds cored with gypsum occur along the River bottom (Baker, 1946, p. 101-103; Lewis and Campbell, 1965, p. B7), attesting to the flow of the gypsum.

The youthfulness of the structures also supports Baker's hypothesis indirectly in that if the graben pre-dated final downcutting by the Colorado River, the proposed mechanism would be impossible. There is much evidence of youthfulness, particularly in the drainage. Much of the area now has internal drainage, yet the remains of an older, integrated drainage are still clearly preserved between the graben. Figures 27 and 28 illustrate some of these drainage relationships.

In a pre-faulting valley on the divide between Cyclone

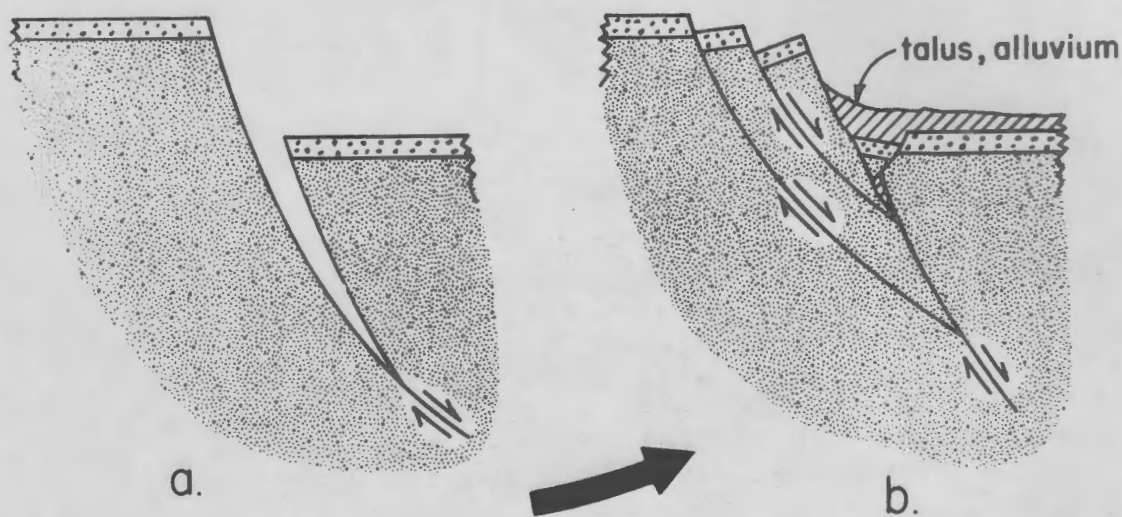


Figure 17: Secondary structures expectable along graben walls where curved, inward-dipping faults occur. This is probably what most geologists would consider "normal", and appears to be the best explanation for secondary structures on most lunar and martian graben as well as most terrestrial graben. Unlike rotation inward toward graben axis resulting from secondary faulting in Canyonlands (Fig. 16), secondary fault blocks are rotated outward away from graben axis by these curved, inward-dipping faults.

---

Canyon and Devils Lane (Fig. 28b) there is a small but sharp anticline paralleling the old valley floor (Figs. 29 and 30). This fold is confined to the region near the pre-faulting creek bed; it does not extend either upward or downward in the section. When faulting occurred, the old stream channel apparently acted as a notch in the horst block. The channel was thus an irregular free surface that permitted localized buckling of the near-surface rocks. Here, as with the Meander Anticline (Fig. 25) and the anticline following Butler Canyon

Figure 18: Joint-bounded segment of graben wall that has dropped several meters and rotated inward towards the graben floor. Arrows point to corresponding beds on rotated block and in main graben wall. The structure at this locality corresponds approximately to that shown in Fig. 16d. West wall of Red Lake Canyon from Spanish Bottom trail.

Figure 19: Upper surface of inward rotated block of Cedar Mesa sandstone. Toadstool caps on dipping surface in foreground correlate with those on skyline. Geometry here corresponds with that shown in Fig. 16c. Red Lake Canyon near junction with Chesler Canyon, looking southwest.



Figure 20: Elongate depression where internal drainage follows joints into subsurface.

Figure 21: Similar to Fig. 20 except depression is nearly circular and crater-like. Note sage brush for scale.

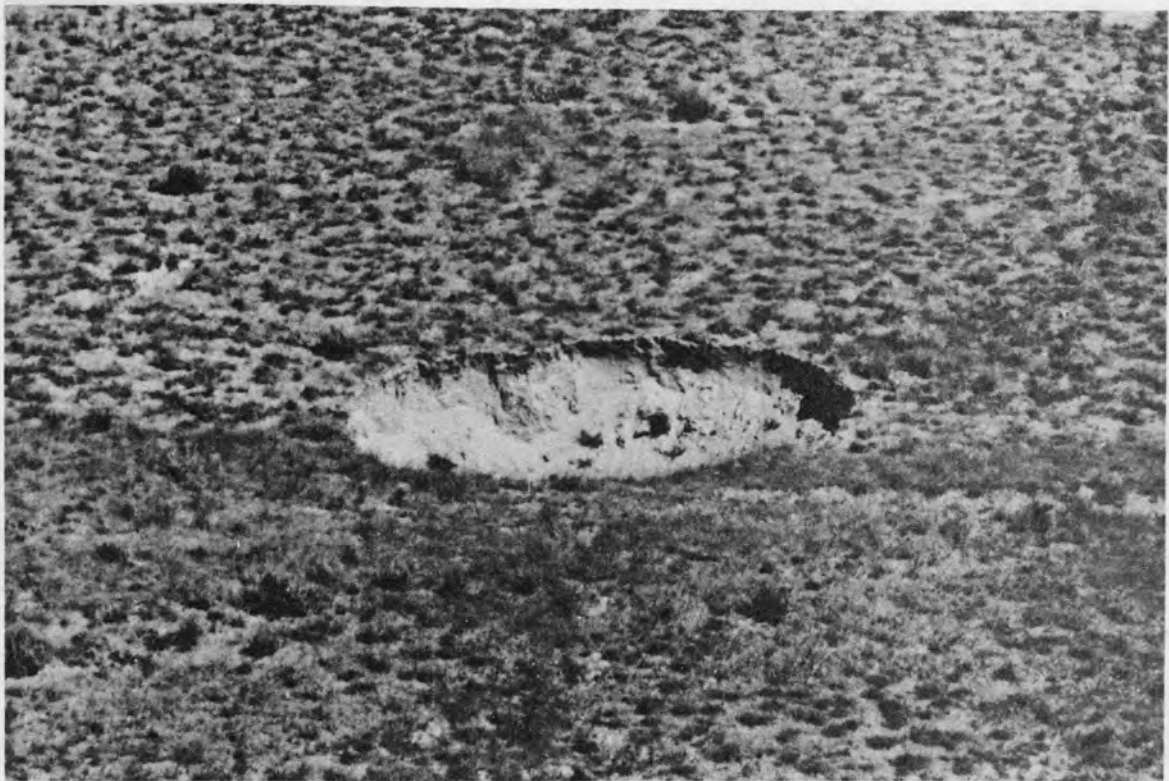
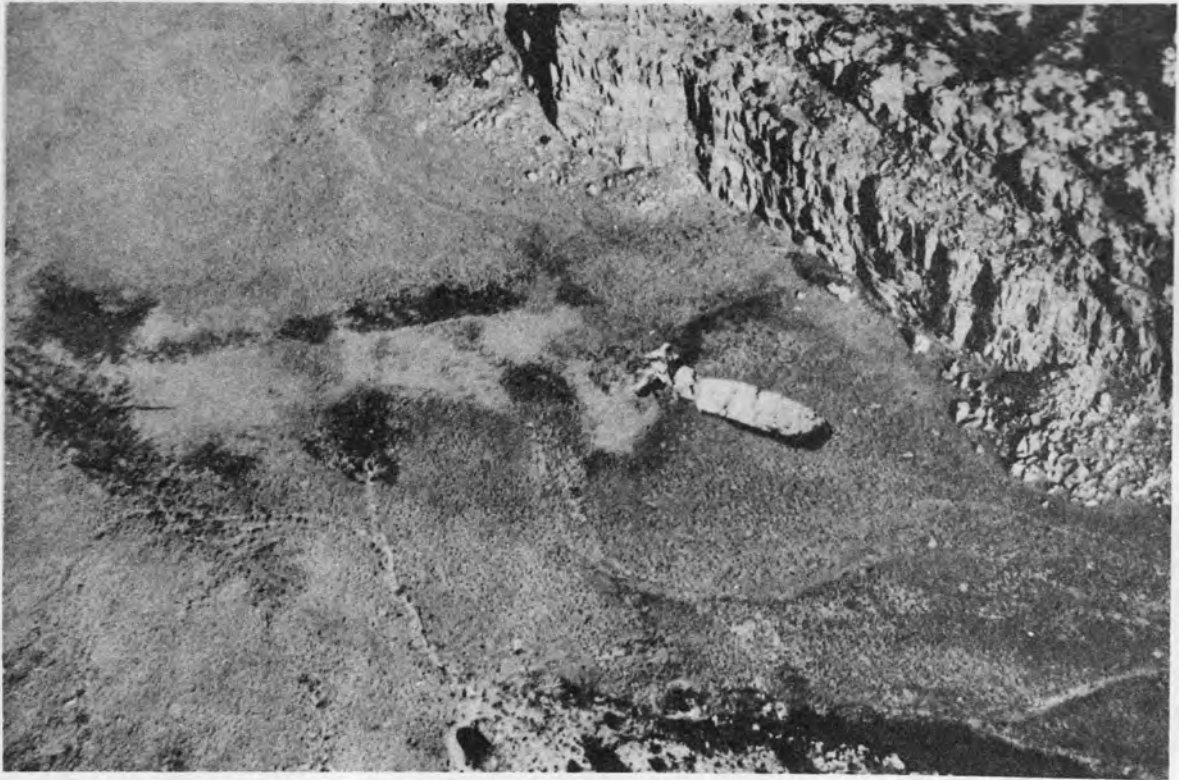


Figure 22: Irregular trace of east wall of Red Lake Canyon graben near its northern terminus. Sawtooth effect is due to non-parallelism of underlying graben trend and strikes of near-surface vertical joints. Looking southwest at junction of Lower Red Lake Canyon and Red Lake Canyon.

Figure 23: Effect of non-parallelism of north end of Cyclone Canyon graben and near-surface vertical joints in Cedar Mesa sandstone. Sawtooth boundary of graben is evidence for independence of graben trends and strikes of earlier joints. Looking south-southwest. Note truncated, pre-faulting east-west valley on inter-graben divides just above center of picture.

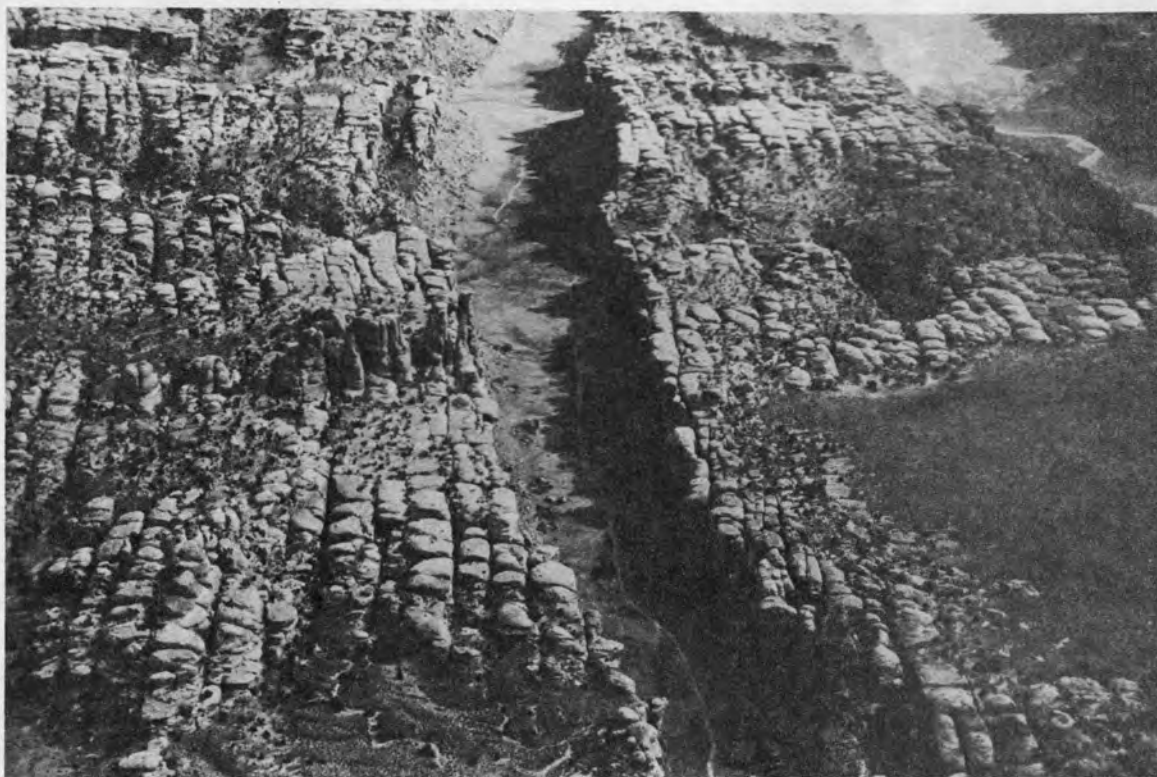
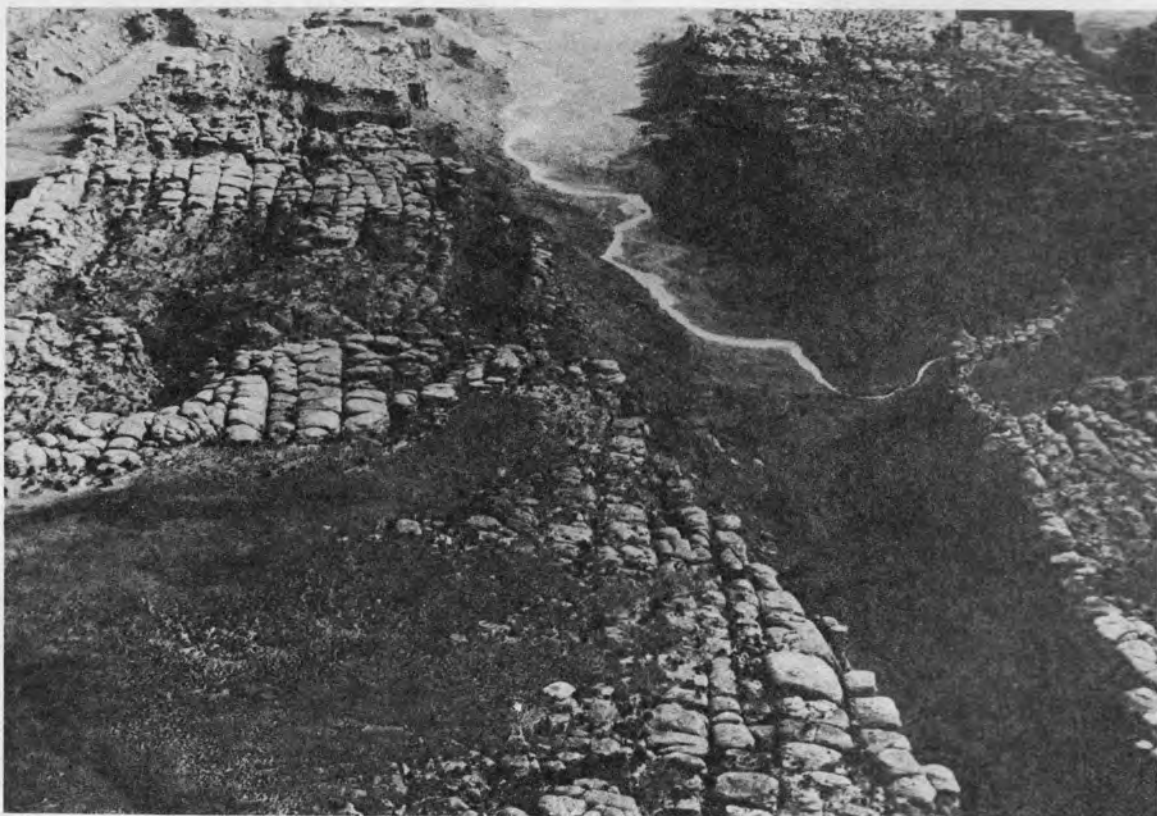


Figure 24: Reversal of regional dip near Colorado River. Looking northeastward at area between Red Lake Canyon (RLC) and Cataract Canyon (CC). The transverse canyon across the center of the photograph is Lower Red Lake Canyon. The regional dip from right to left is so gentle as to be imperceptible except when standing directly on the upper surface of the Cedar Mesa Formation on the inter-graben divides. The dip reversal in the left portion of the photograph is sufficiently pronounced to be visible in this oblique view.

Figure 25: Looking west across Cataract Canyon at western flank of Meander Anticline. Note restriction of significant dip to immediate vicinity of the river canyon. Associated graben (not visible) are also restricted to the immediate vicinity of the river.



(Fig. 26), it is difficult to separate structural geology from geomorphology!

The correspondence of structural details to the stream valleys at all scales argues strongly for a close relationship between drainage development and structural evolution. If the faulting had pre-dated the Pleistocene, a time of moister climate and more rapid erosion, the drainage would have had ample time to adjust and re-integrate. Thus, the good preservation of abandoned drainages, and the persistence of internal drainage argue for the youthfulness of the present drainage, and thus for the youthfulness of the faulting.

Hunt (1969, p. 67, 127) estimates an erosion rate of 3 to 6.5 inches per 1000 years for the Colorado River as a whole during the recent past. The River has cut about 100 to 200 feet into the Paradox Member in Cataract Canyon (Lewis and Campbell, 1965, Plate 2), hence we can calculate that the time since the River reached the upper contact of the Paradox is between 200,000 and 800,000 years. However, flow of the gypsum almost certainly began before the river actually cut down to it. The anticline in Lower Red Lake Canyon (Fig. 26) persists upstream to a point where the Paradox Member is about 150 feet beneath the level of its bed. Using this depth as an estimate of the distance from the Colorado River bed to the Paradox when flow began, the estimated time since gypsum flow began is 500,000 to 1,400,000 years. On the other hand, the river gradient in Cataract Canyon is much steeper than average (Hunt, 1969, p. 101), suggesting a more rapid rate of



Figure 26: Anticline trending parallel to Lower Red Lake Canyon, looking west (downstream). At the level of the dry river bed, the anticlinal trace follows the meanderings of the valley. Arched rocks are in the Hermosa and Rico Formations. West wall of Cataract Canyon in the background also exposes massive cliffs of Cedar Mesa Formation topped by needles of Organ Rock Tongue.

-----

downcutting than the average for the whole river. Finally, the upward motion of the gypsum in the canyon probably causes an over-estimation of the depth of erosion into the Paradox Member. Both of these last sources of error produce over-estimates of the time since flow began, but it is difficult to estimate the magnitude of the errors. Considering all the possible causes for error either way, the most probable time

since initiation of graben faulting is on the order of 500,000 years. This figure is not likely to be off by more than a factor of 3. Lewis and Campbell (1965, p. B31) report minor movements on some of the faults in historic time which, with some of the drainage characteristics, suggest that lateral flow and graben faulting are still going on.

## EXPERIMENTAL SIMULATION

### Introduction

We have used scale-model experiments to investigate the behavior of brittle materials overlying a "viscous" layer free to flow down a gentle slope. Figure 31 illustrates the model apparatus. Various thicknesses of dry sand, ground limestone, and sand mixed with ground limestone were spread over the flowing layer (paraffin) to simulate brittle layers with different properties. Dry sand responds to stresses by developing shear planes inclined at about  $30^\circ$  to  $\sigma_1$  (compressive stresses positive) (Hubbard, 1951). In our experiments, the ground limestone failed along vertical fractures that were either shear planes or were planes perpendicular to  $\sigma_3$ . Thus, a layer of dry sand overlain by a thinner layer of ground limestone should produce a fault geometry similar to that believed to exist in Canyonlands (Fig. 8d). We were pleased to find that these experiments produced model graben possessing many characteristics in common with the prototypes.

For many reasons related to problems of scaling size,

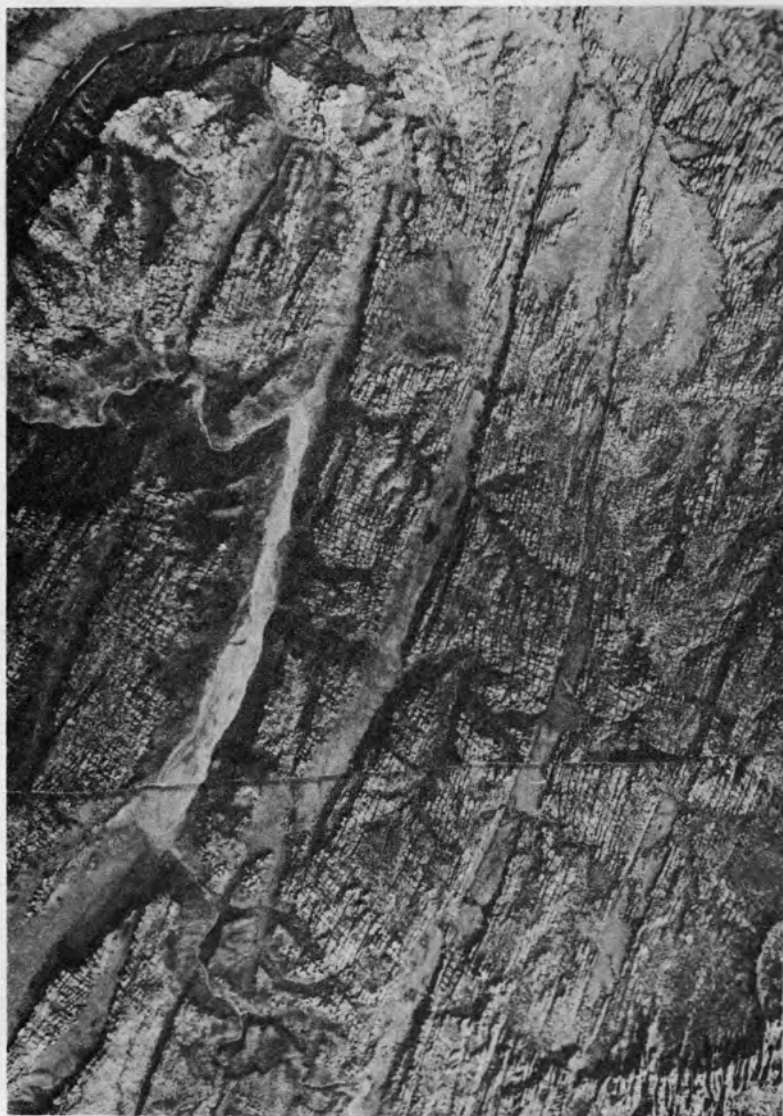


Figure 27: Mosaic of vertical aerial photographs of a portion of the Canyonlands graben complex illustrating contrasts between pre- and post-faulting drainage patterns. The changes in drainage of this area are sketched in Fig. 28.

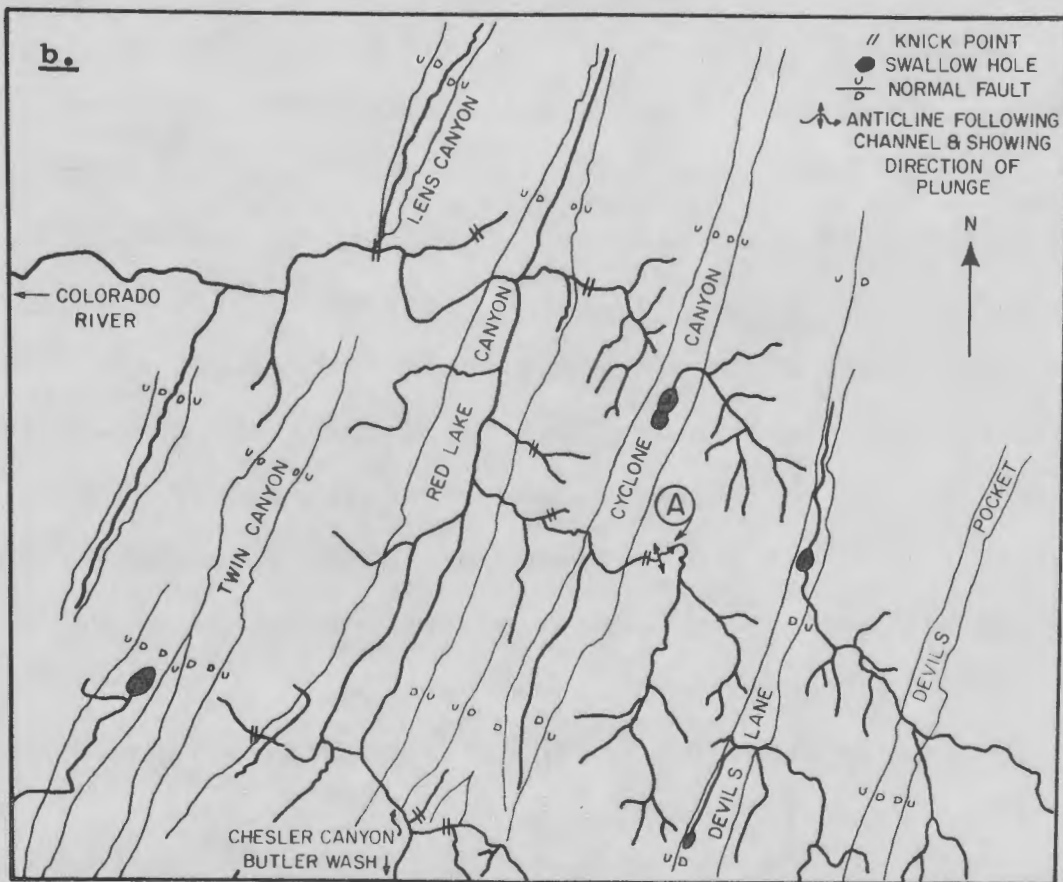
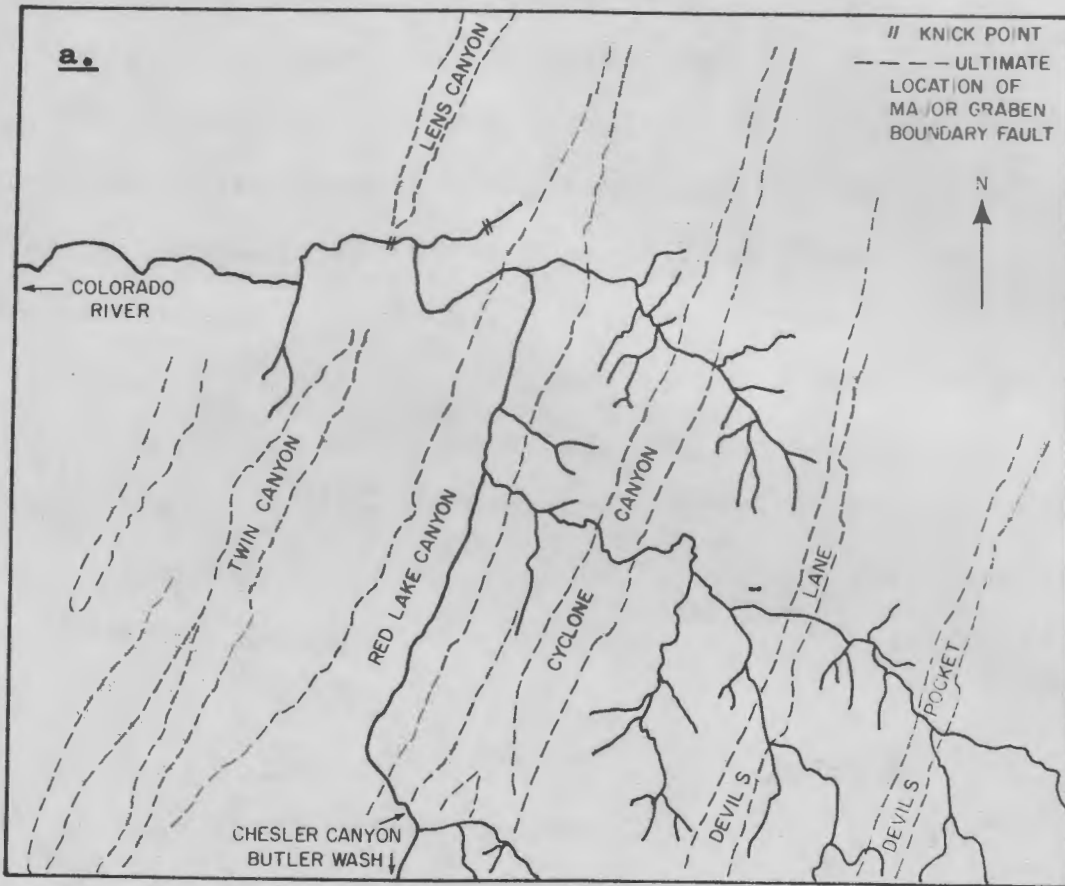
-----

material properties and time, and to the validity of boundary conditions, the results of model experiments can never be applied in a direct, quantitative way to the origin of natural

Figure 28: Changes in drainage due to graben faulting.

a. Drainage prior to faulting, inferred from remnants surviving on inter-graben divides. Future sites of major graben faults shown by dashed lines. Stream pattern suggests partial joint control of drainage, supporting the inference from structural analysis that joints pre-date graben faulting. If joints were as prominently expressed in the topography prior to faulting as now, one would expect the stream pattern to have been more rectangular than shown in this figure. Thus, this pre-faulting drainage pattern suggests that, though present prior to faulting, the dominant joint sets were not as wide open then as they are now.

b. Present drainage. Pattern is superficially the same as before faulting, but individual valleys have been disrupted. Many of the ephemeral streams now terminate within graben, either at a swallow hole or simply at the low point within the fault valley. Knick points on inter-graben divides record extent of headward erosion since faulting. A = small drainage-controlled anticline (Figs. 29 and 30).



structures. As has been observed by others (cf., Johnson and Pollard, 1973, p. 281-282), scale models are useful for the geometrical insights they provide. It is also interesting to investigate the general dependence of one parameter on another. Unfortunately, it is possible for an effect to have more than one cause, and it is thus possible that the cause investigated experimentally is not the one which operated in the natural prototype. The results summarized below should be interpreted qualitatively, and should be used for their geometrical insights only.

#### Experimental Results

Figures 32 through 41 illustrate the results of two of our experimental runs. The only initial difference between the two was the thickness of the sand layer. The top layer of ground limestone developed a visible network of vertical shear fractures in experiment 2 (Figs. 32-36). When the graben formed later in the experiment, the bounding faults followed these fractures in the limestone layer (Fig. 36), producing a sawtooth effect similar to that shown in Figs. 22 and 23. In the sand layer, the faults have trends that are clearly independent of the fractures in the ground limestone. These faults in the sand are inclined inward toward graben troughs. The overall geometry produced in experiment 2 is a result of the following chronology:

1. Early shear fracturing of the surface layer, implying that  $\sigma_2$  is vertical in that layer.

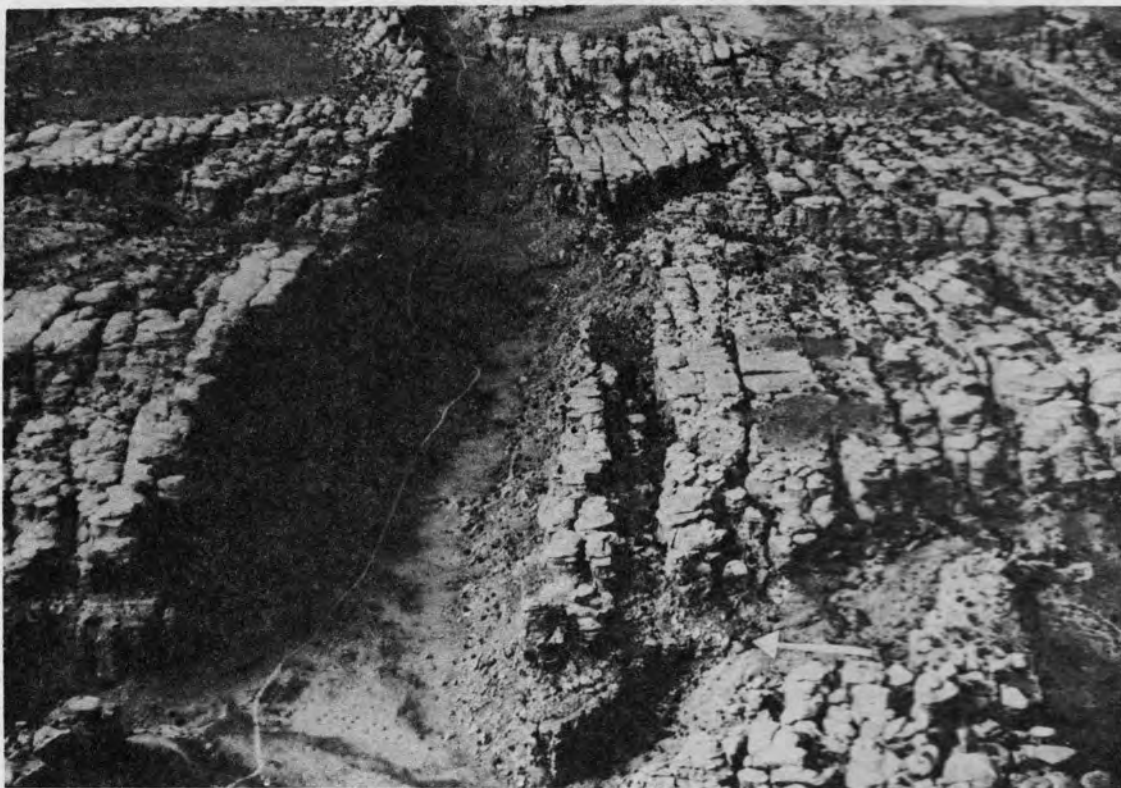


Figure 29: Cyclone Canyon graben, looking north. Drainage extending to right (upstream) of Cyclone Canyon from lower edge of photograph has a pronounced knick point (arrow). Immediately above this knick point is a small anticline confined to the vicinity of the valley floor (Fig. 30).

-----

2. Development of graben in the sand, with steep inward-dipping bounding faults, implying that  $\sigma_1$  is vertical at the level in the sand where faulting initiates (most likely at or near the sand/paraffin contact).

3. Upward propagation of the inclined faults in the sand layer until the contact with the limestone layer is reached, above which the fault motion follows the pre-existing shear

fractures in the limestone, producing a sawtooth pattern in plan view.

Experiment 4 (Figs. 37-41) does not show the shear fractures visible in experiment 2, but the tendency for the margins of the graben to be sawtoothed suggests that shear fractures are present though not visible. We do not know yet what controls the degree of development of the shear fractures. The graben in Figs. 40 and 41 illustrate some secondary structures very well. Both types of rotation on secondary faults illustrated in Figs. 16 and 17 are present. Blocks rotated inward toward the graben axis, involving only the vertically faulted limestone layer, are present along the outer margins of the graben. Outward rotated blocks, apparently dropped on inclined faults in the sand, occur closer to the axis of the graben. These model graben are structurally more complex than most of the Canyonlands graben where we see only inward rotated blocks, presumably because our field observations to date are entirely confined to the near-surface layer of vertical faulting.

#### Conclusions from Model Studies

1. Lateral flow of a "viscous" layer can result in graben in overlying brittle layers. Although details vary, the existence of graben is not sensitive to values of parameters we have varied (flow rate, thickness of brittle layers, composition of brittle layers, lateral boundaries on model, thickness of flowing layer above minimum necessary for flow to



Figure 30: Small anticline along pre-faulting creek bed on divide between Cyclone Canyon and Devils Lane, looking downstream toward Cyclone Canyon. Note man for scale in upper left portion of photograph. Dips on flank of this small anticline range from  $23^{\circ}$  to  $51^{\circ}$ . The fold cannot be traced away from the vicinity of the old valley floor laterally or vertically. Such close correspondence between valley floors and folds argues for geomorphic control of folding. A corollary of this is that the folds cannot have formed before the drainage developed.

occur), at least within the limits so far investigated.

2. Graben faults apparently begin in the brittle material immediately above the flowing layer and propagate upward to the surface. If near-surface materials are strongly anisotropic, the orientations of the upward-propagating faults may be affected. A similar sequence was derived from field evidence in Canyonlands National Park before the experiments were run.

3. The experimental graben support the suggestion implied by Figs. 16 and 17 that the nature of rotation on secondary fault blocks is a clue to the attitude of the primary faults bounding the graben.

4. The boundary and flow conditions of the model are very similar to those postulated for a valley glacier, a comparison that will be pursued in the next section of this report.

## THEORETICAL ANALYSIS

### The Glacier Flow Model

Nye (1951, 1952, 1957, 1965) has developed a quantitative theory of glacier flow by assuming that the stresses in a glacier which is flowing in a steep-walled valley of simple rectangular shape may be approximated by superposing variable shear stresses on normal stresses that are constant for any depth in the ice. He has extended the analysis to valleys of non-rectangular shapes, but these are of little interest here.

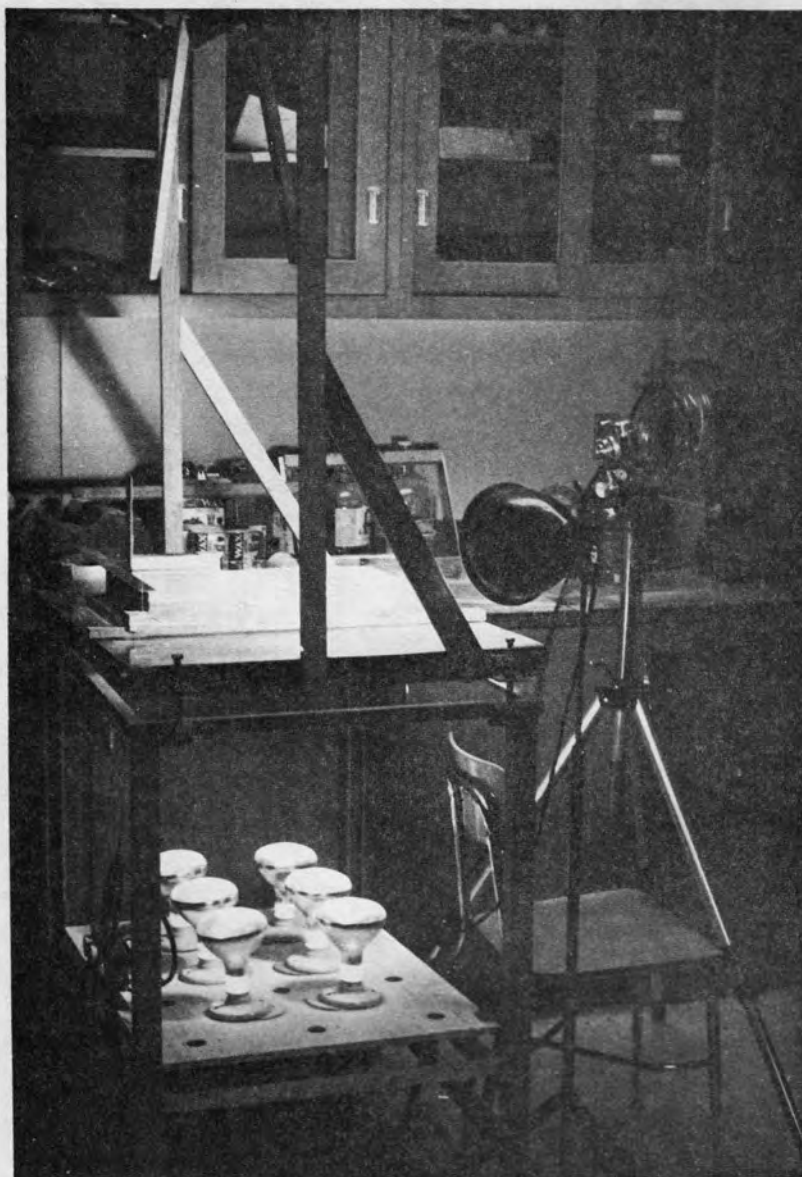


Figure 31: Apparatus used for scale-model experiments. Frame at top is for camera used to take overlapping vertical photographs. Frame used to confine paraffin, sand, and ground limestone rests on glass top of table. Large bulbs are rheostatically controlled heat lamps used to soften the paraffin, which then flows down the tilted glass top, deforming and faulting the sand and ground limestone. Rate of flow may be controlled by varying the heat output from the lamps or by varying the tilt angle of the glass top. The lamps are mounted on a hinged board and may be rotated clear of an underlying camera (not visible) used to photograph the bottom of the flowing paraffin through the glass table top.

Figure 32: Experiment 2 prior to test. Materials within frame are, from surface of glass upward, 16mm of paraffin, 20mm of dry sand, and 2mm of ground limestone. Dimensions of test mass: 40cm x 50cm. Tilt angle of glass table top = 2°. Lines trending across model are trowel marks.

Figure 33: Experiment 2 after 1 hour and 56 minutes. Flow direction in paraffin is to the right. Note development of grid of curved fractures in ground limestone layer.

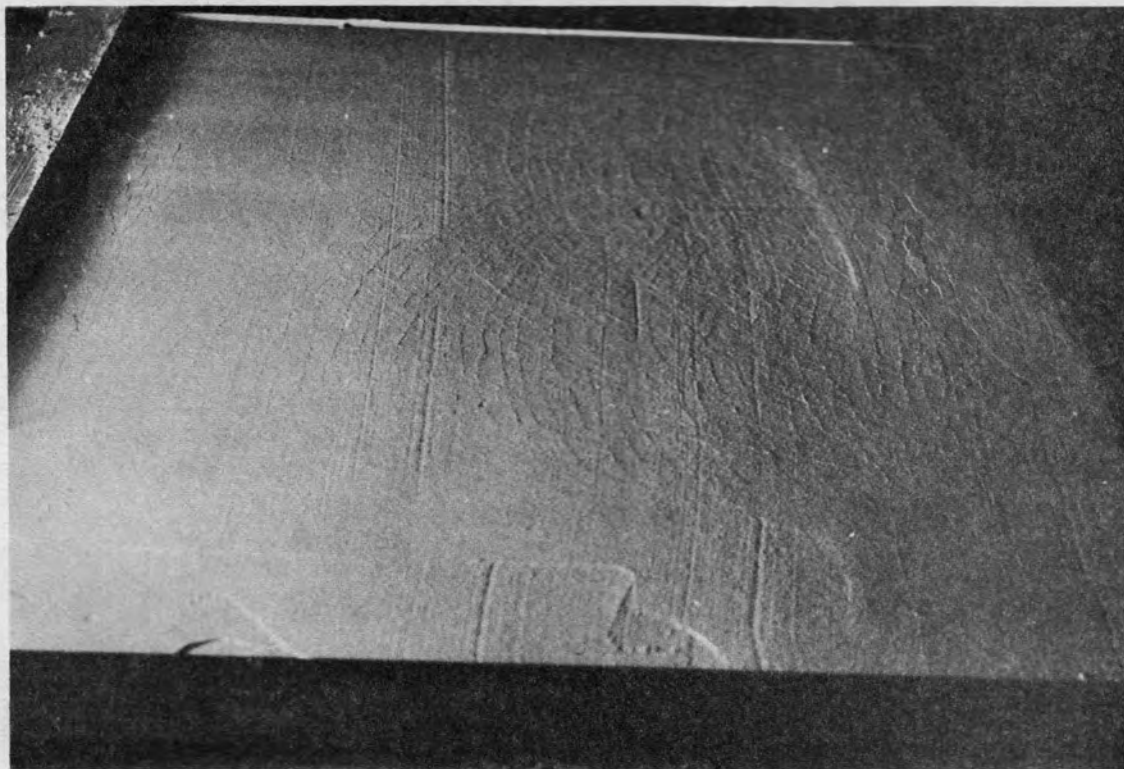
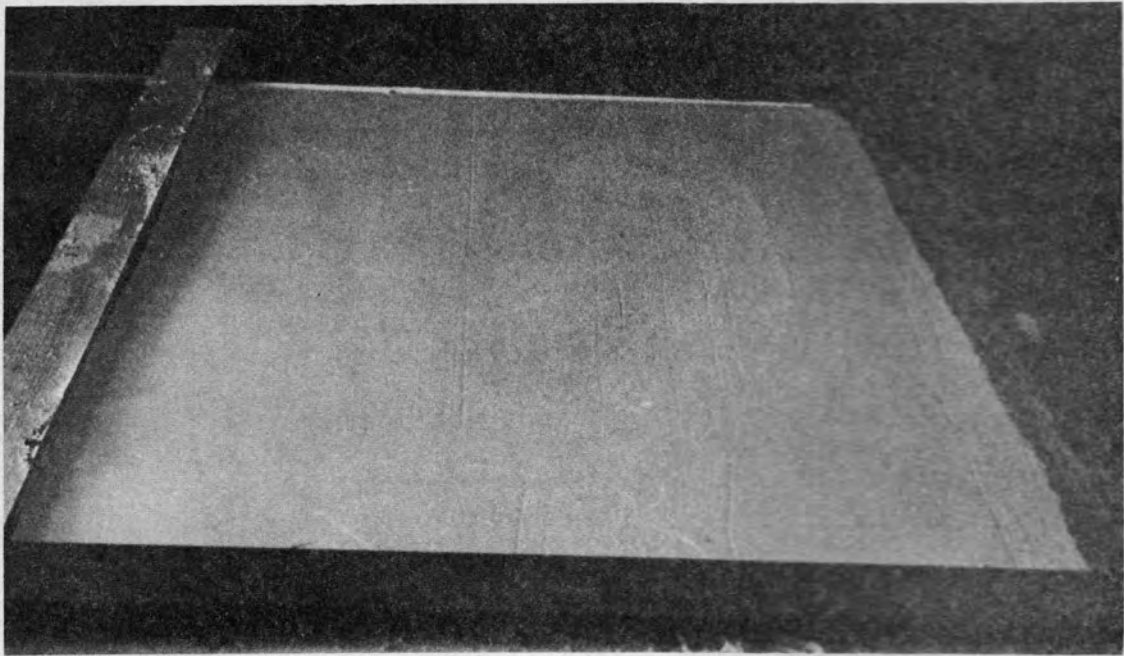
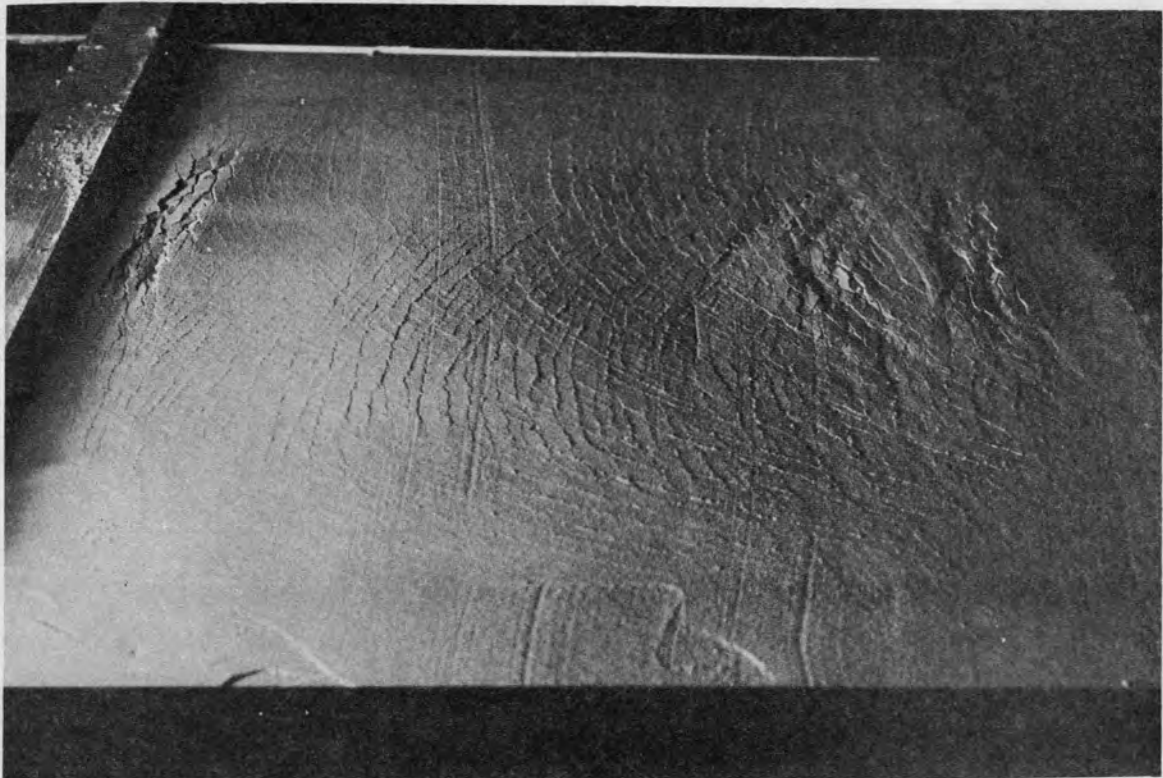


Figure 34: Vertical view of relationship shown in Fig. 33. Flow direction is toward top of page. Light source is at a very low elevation angle to enhance fractures by shadowing; there is very little movement on the fractures at this stage. The fractures are vertical, and are interpreted as shear planes, implying that  $\sigma_2$  (compressive stresses positive) is normal to the model surface in the limestone layer when they form. See Fig. 44a for interpretation of stress trajectories.

Figure 35: Experiment 2 after 2 hours and 9 minutes. Note beginnings of graben at right which do not trend parallel to earlier-formed shear fractures. Graben at left is related to confined "upstream" boundary of model, and is not used in any of the analyses which follow.



By creating transverse marker lines in the paraffin with dyes, we have been able to monitor the displacement of the paraffin (Fig. 42) and demonstrate that the transverse distribution of flow is roughly analogous to that in a valley glacier (Meier, 1960, Fig. 42; Nye, 1965, Fig. 6c). Variations in the specific deformed shape of an originally straight transverse line in the flowing material depend on material properties, boundary conditions, and the sign and magnitude of superposed longitudinal normal stresses. Nye's quantitative models all show a non-linear increase of shear stress near the surface of the glacier from 0 at the glacier mid-line to a maximum value near the periphery. The exact form of this stress increase, and the position of the stress maximum relative to the periphery of the glacier depend on the channel shape assumed.

Boundary conditions, material properties, and flow patterns of our experimental models are analogous to those of a valley glacier in extending flow confined in a simple rectangular valley. Hence we believe it reasonable to assume the same semi-quantitative stress distributions assumed by Nye (1952, p. 89-91) to explain the failure of brittle near-surface material under such conditions.

#### Application of Glacier Model to Scale-model Experiments

Figure 43 illustrates the stresses acting on the sand and crushed limestone layers of our models, assuming that the analysis for extending flow given in Nye (1952, Fig. 9c) may be applied to the ductile paraffin layer. Figure 44a illustrates

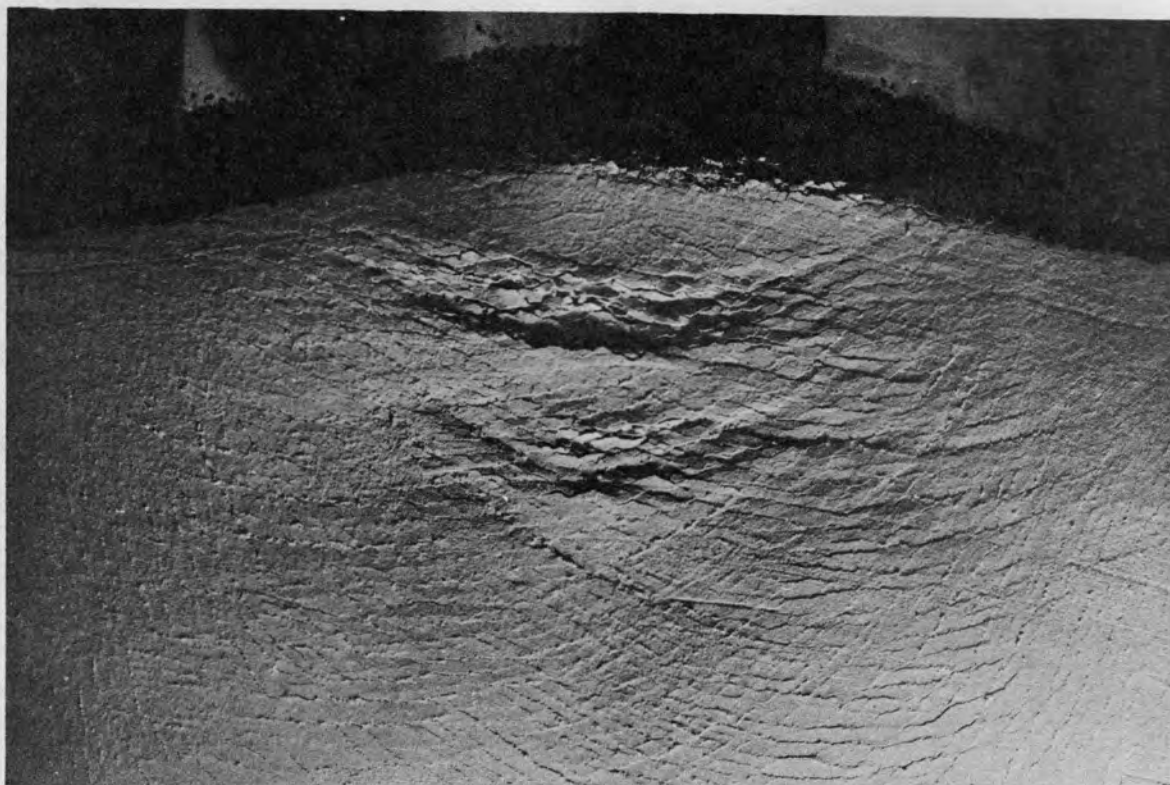


Figure 36: Experiment 2 after 3 hours and 15 minutes. Flow direction in the paraffin is toward the top of the page. The graben clearly have trends independent of the early shear fractures formed in the ground limestone (Fig. 44b). The two fracture trends interact in the limestone layer to produce a saw-tooth effect reminiscent of that seen near the northern ends of the graben in Canyonlands (Figs. 22 and 23).

---

the expected orientations of principal stresses and shear fractures near the top surface of the model materials assuming that the stresses due to flow are of sufficient magnitude that  $\sigma_1$  and  $\sigma_3$  (compressive stresses positive) are both in the plane of the layering (in the absence of flow, of course,  $\sigma_1$  must be vertical). Presumably at some depth in the brittle

Figure 37: Experiment 4 prior to test. Materials within frame are, from surface of glass upward: 16mm of paraffin, 45mm of dry sand, and 2mm of ground limestone. Dimensions of test mass: 40cm x 50cm. Tilt angle of glass table top = 2°.

Figure 38: Experiment 4 after 50 minutes. Flow direction in paraffin is to the right. Note formation of complex curved graben without prior development of visible shear fractures in limestone layer.

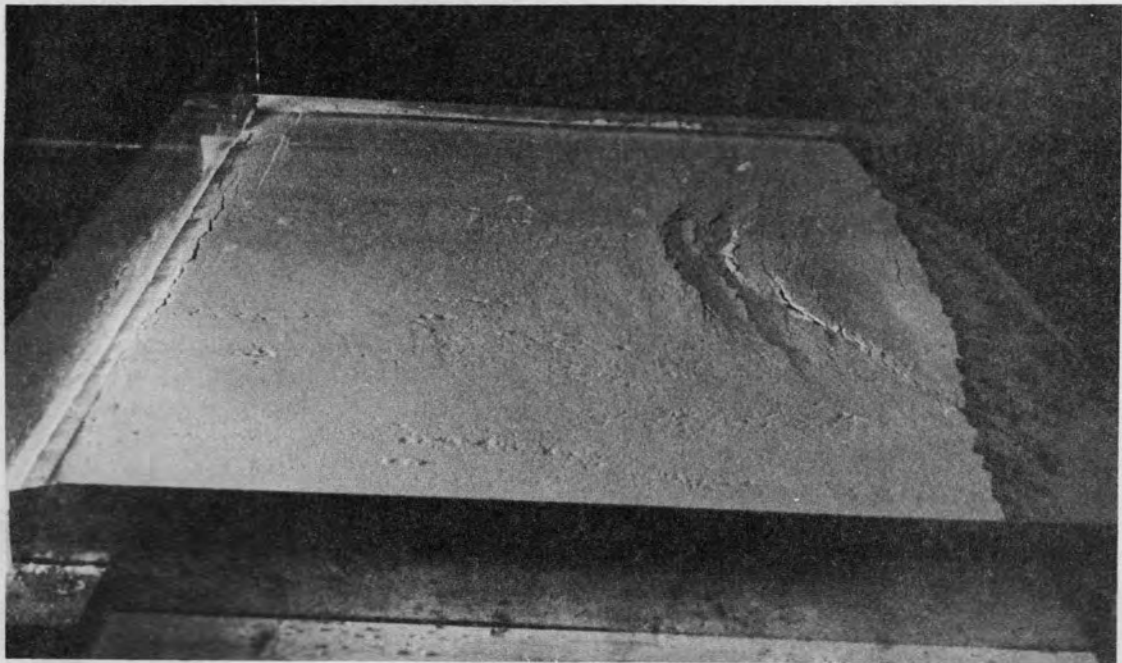
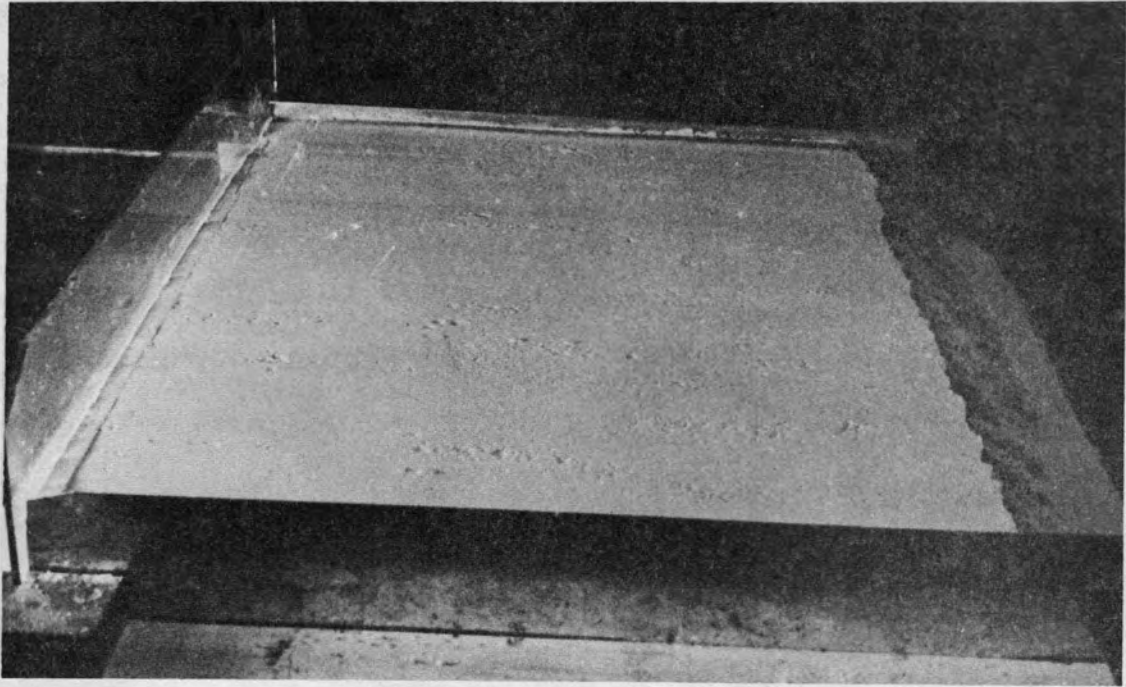


Figure 39: Experiment 4 after 2 hours and 11 minutes. Original graben continues to get more complex, and a second graben begins to form farther "upstream." Note reversal of dip of surface near free edge at right where flowing paraffin moves upward as well as laterally.

Figure 40: Experiment 4 after 3 hours and 53 minutes. Note contrasting rotation directions of detached and dropped slabs. Along right margin of younger graben is a line of limestone slabs that have separated from graben wall along a vertical fracture in the ground limestone and have rotated inward, toward the axis of the graben, analogous to what is seen in Canyonlands (Figs. 16 and 19). Within the older graben are two lines of larger tilted slabs that have rotated outward away from the axis of the graben along inward-dipping fractures in the underlying sand layer (Fig. 17). Figure 49 presents evidence for similar outward rotation in a martian graben.

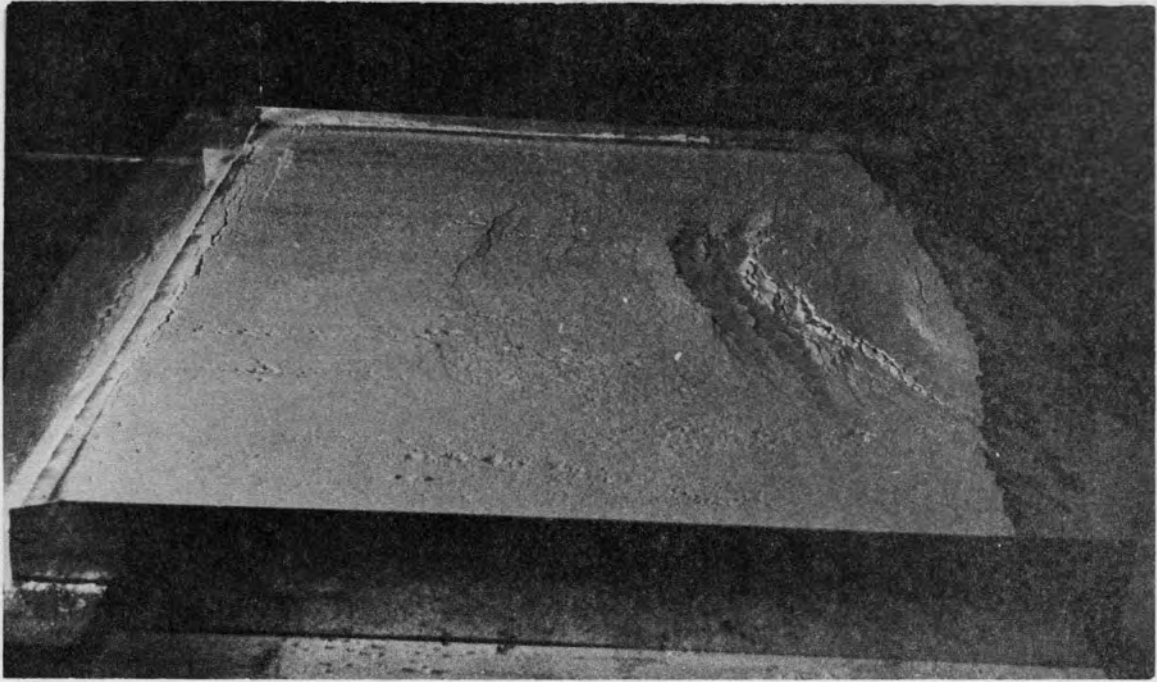


Figure 41: Like Fig. 40, but viewed vertically. Flow direction in paraffin is toward the top of the page. Note again the contrasting rotation directions of lines of detached and dropped slabs. Poorly developed, but nevertheless apparent sawtooth effect along graben faults suggests that early shear surfaces did form in the limestone layer but that they did not develop sufficiently to become visible.

Figure 42: Deformation of originally straight transverse lines of dye in paraffin after 3 hours of flow.

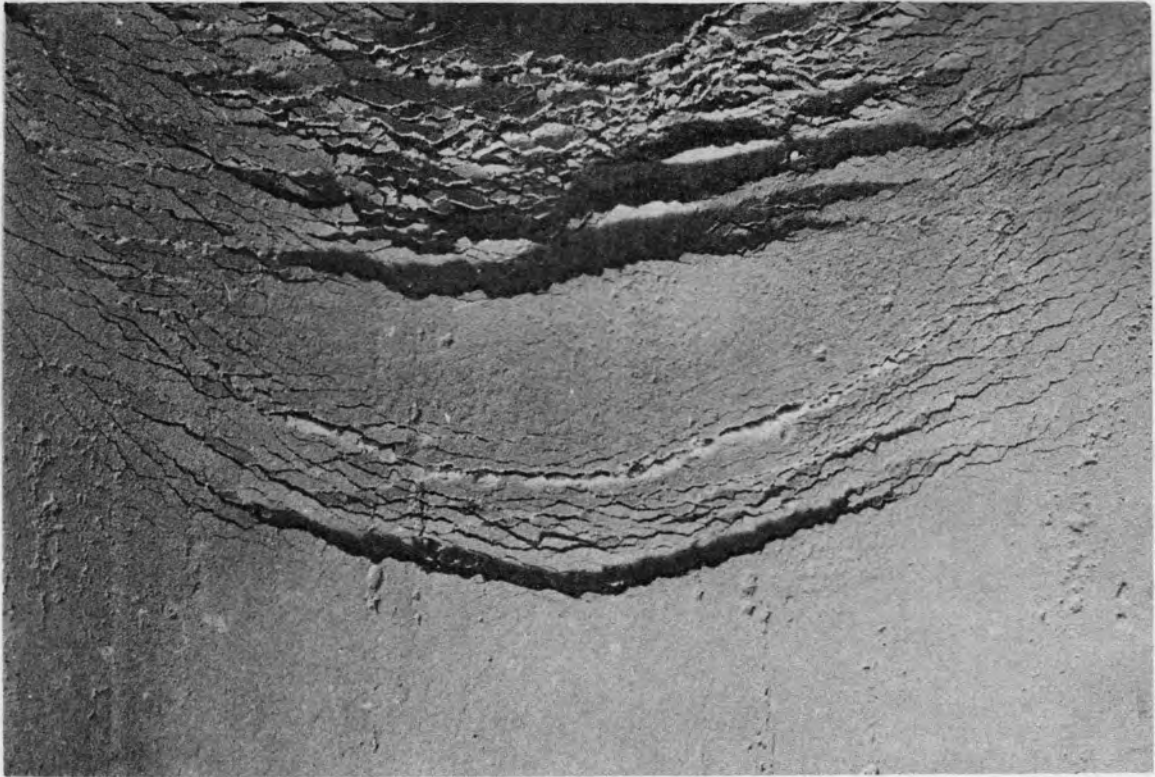
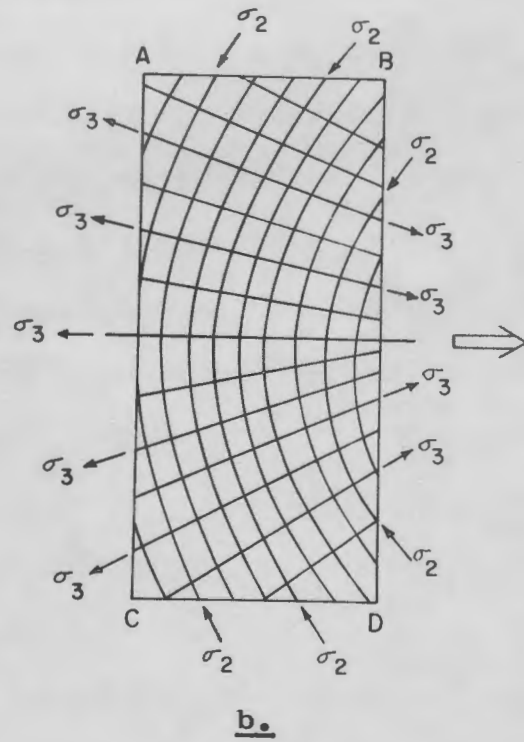
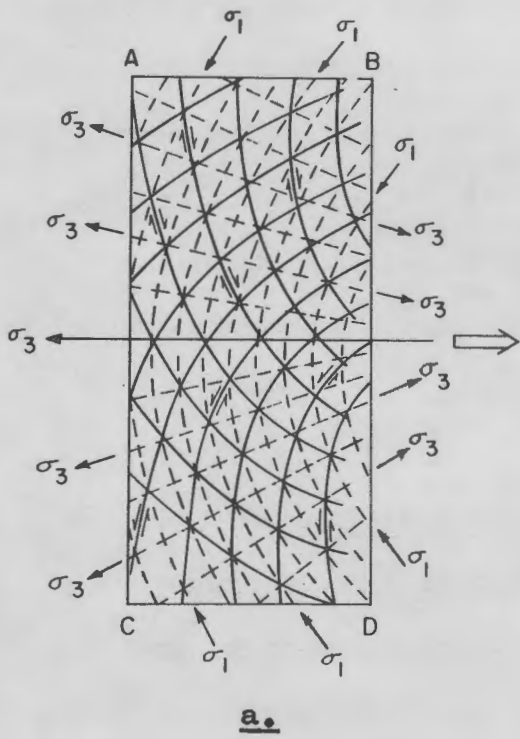
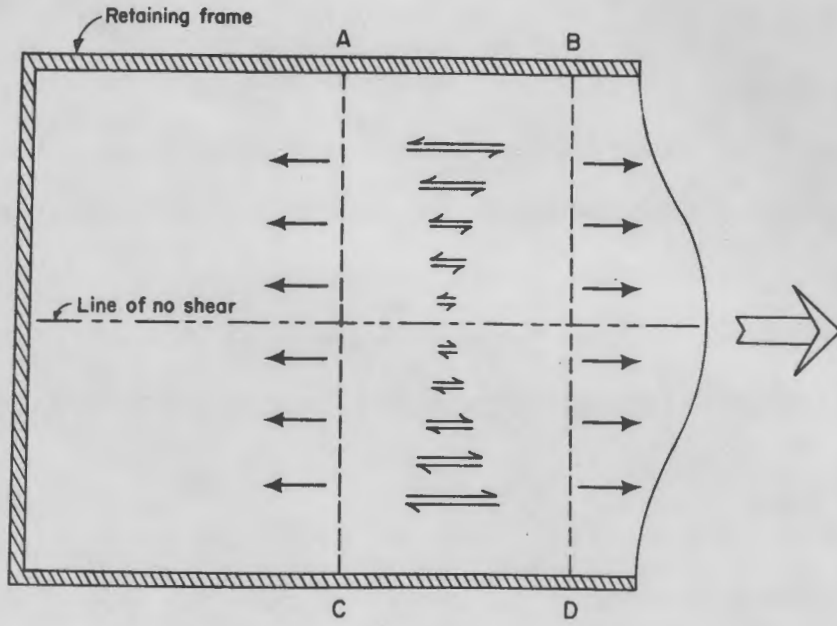


Figure 43: Stress model for a valley glacier in extending flow (Nye, 1952) applied to model experiments. Assumed stresses shown acting on an arbitrary rectangular volume of material ABCD. Center line is the trace of a vertical plane of no shear; shear stress increases symmetrically from this line to maxima at the boundaries of the model. Tensile stress assumed to be constant across glacier (and model). This tensile stress in the direction of flow implies a smaller transverse tensile stress due to constant model width. This transverse stress is not shown, nor is the roughly hydrostatic compression that exists due to gravity. The shear stresses shown must be balanced by other shear stresses acting on transverse planes in order to assure that the sum of moments is zero. These stresses also are not shown.

Figure 44: Principal stresses at two levels in the model, resulting from superposition of stresses acting on volume ABCD in Fig. 43. Compressive stresses are considered positive.

a. In the ground limestone layer near the surface of the model. Stresses superposed by flow of the paraffin are of sufficient magnitude, and the weight of overburden sufficiently small, that  $\sigma_1$  is parallel to the layer rather than approximately vertical. Dashed lines are trajectories of  $\sigma_1$  and  $\sigma_3$  in the plane of the limestone layer.  $\sigma_2$  is approximately vertical. Solid lines are traces of vertical shear planes, assuming that the planes most likely to fail in shear lie about  $30^\circ$  either side of  $\sigma_1$ . Early formed fractures in experiment 2 (Fig. 34) have orientations corresponding closely to these theoretically predicted shear planes.

b. In the sand layer, sufficiently deep that the weight of overburden compels  $\sigma_1$  to be vertical. Lines are trajectories of  $\sigma_2$  and  $\sigma_3$  at some arbitrary depth in the sand. The trends of the major faults bounding the graben in both experiments (Figs. 36 and 41) are parallel to the  $\sigma_2$  stress trajectory, as is predicted by Anderson (1951).



material the stress due to gravity becomes sufficiently large to compel  $\sigma_1$  to be vertical despite the superposed horizontal stresses due to flow in the underlying paraffin. Figure 44b illustrates the orientations of principal stresses in layers where  $\sigma_1$  is vertical. These two principal stress orientations correspond to the "strike-slip fault" and "normal fault" cases in the simplified mechanical theory of faulting (Anderson, 1951, p. 13-16).

A comparison of Fig. 44 with Figs. 32 to 41 illustrates the close correspondence between the glacier model stress trajectories and the orientations of the experimentally produced fractures and faults. The pattern of early shear fractures in experiment 2 (Fig. 34) closely matches that predicted from the glacier model for shear planes near the surface. Likewise, the curved trends of the graben faults correspond closely to the trajectories of  $\sigma_2$  predicted from the glacier model to occur at depths sufficient for  $\sigma_1$  to be vertical. It is important to note that the curvature is a function of boundary conditions. In an infinitely wide glacier or scale model the stress trajectories would be straight.

#### Validity of Glacier Model for Canyonlands Graben

Because the gypsum can flow toward the Colorado River only where the river has trenched deeply enough to expose (or nearly expose) the Paradox Member, the 25Km long block of moving rock has lateral boundaries that are mechanically analogous to the boundaries of a valley glacier, even if geometri-

cally different. Thus the presence of the Canyonlands graben, and their curvature, can be accounted for by the valley glacier stress model. This model also predicts that the inclined graben faults should be initiated at some depth rather than at the surface, consistent with the model derived solely from field evidence.

We are very reluctant to apply the glacier model to the early formed vertical joints in the Canyonlands, tempting as this might be. In the model experiments, the early vertical shear fractures are clearly due to the same stress field as the slightly later inclined normal faults defining the graben. A number of facts argue against explaining the orientations of the Canyonlands joints as due to the same stress field as the graben. These include:

1. The joint sets are areally much more extensive than the graben.
2. The shear fractures predicted by the model do not form sets at  $90^\circ$  to each other, but the joint sets in the Canyonlands area intersect at angles very close to  $90^\circ$ .
3. Mutually perpendicular sets of vertical joints are found in many places in the world, and hence cannot generally be due to such a special set of circumstances as exist in the Canyonlands.
4. For a significant proportion of their length, the graben of Canyonlands are nearly parallel to one joint set, which is not in accord with either the glacier model or the experimental results.

Because rectilinear joint sets are so common, it seems most likely that the ones at and near Canyonlands pre-date the entire stress field responsible for the graben, but that the stresses set up by lateral flow on the gypsum utilized these earlier joints to break up the near-surface rocks. The near parallelism of the graben system with one joint set is probably due to joint control of the north-northeast-trending Cataract Canyon portion of the Colorado River, guaranteeing that gypsum flow, and hence  $\sigma_3$ , would be about normal to one joint set.

These interpretations are clearly oversimplified because there are many details of the joint pattern that do not fit. We hope that continuing studies of the fracture pattern will resolve some of these problems.

#### DISCUSSION AND CONCLUSIONS

Some of the geometric peculiarities of the Canyonlands graben seem to be related to the vertical dip of the bounding faults in the near-surface rocks. It is interesting to speculate on the significance of this fact and, in particular, whether vertical dips are restricted to Canyonlands or at least to graben of similar size. Figures 45 through 47 show some young faults and extension cracks along the mid-Atlantic rift in the Þingvellir area of Iceland. The faults and fractures are vertical, and the secondary structures are similar to those observed in Canyonlands. The mid-Atlantic rift is



Figure 45: Fractures at Þingvellir, Iceland, looking north. Note buildings for scale. Along largest fracture a line of huge slabs has dropped and rotated inward toward the lower plain, which is a portion of the floor of the mid-Atlantic rift. The geometry along the vertical graben fault, with slabs rotated inward toward the axis of the graben, is remarkably similar to that seen along the wall of the younger experimental graben in Figs. 40 and 41, and is also similar to what is found in many places in the Canyonlands graben complex (Figs. 16 and 19). In all three cases, the master fault is vertical. Clearly, the scale of the structure does not seem to alter the geometric response. Right of the center of the photograph are some large, vertical extension cracks in the materials of the graben floor. Figures 46 and 47 show the largest of these from the ground.

Figure 46: Large extension fracture on the floor of the mid-Atlantic rift at Þingvellir, Iceland, looking north. This is a very simple structure, with no evidence, in this figure, for any secondary faulting. Note in middle distance the inward tilted slabs dropped from the major fracture illustrated in Fig. 45.

Figure 47: Detail near north end of fracture in Fig. 46. Note beginning of a rigidly rotated ramp at end, where the crack is dying out, analogous to the ramps at the ends of the Canyonlands graben. This suggests that the fracture may be better represented as a very narrow graben bounded by vertical faults than as a simple open extension fracture. One would probably estimate a smaller amount of lateral spreading if this is a graben than if it is an open extension fracture. In fact, this figure suggests that very little lateral spreading is needed to produce this fracture.



undoubtedly far more complex than the graben of Canyonlands, hence we do not wish to make too much of these pictures from one small area. They do indicate, however, that vertical boundary faults, and associated secondary structures, are not restricted to the Canyonlands graben, nor apparently to graben within a narrow size range.

The graben of the Tharsis region of Mars vary in size, but generally their widths fall somewhere between the widths of the graben of Canyonlands and the total width of the mid-Atlantic rift in Iceland. They appear to be much more complex than the graben of Canyonlands, and to have been formed at more than one time (D. U. Wise, personal communication). Secondary structures visible at the resolutions of Mariner 9 B-frames are more consistent with inward-dipping bounding faults near the surface than with vertical faults (Figs. 48 and 49). This agrees with evidence for the attitude of faults bounding straight and arcuate lunar rilles (McGill, 1971; Baldwin, 1971).

Field evidence discussed in this report supports the speculations of Harrison and Baker regarding the origin of the Meander Anticline and the graben of Canyonlands National Park, Utah. Clearly, lateral flow of "viscous" material beneath more brittle surface layers is a valid mechanism for the formation of graben. Furthermore, the boundary conditions on the moving block at Canyonlands are mechanically analogous to those on a valley glacier, permitting us to apply stress analyses worked out for glaciers. These stress analyses predict

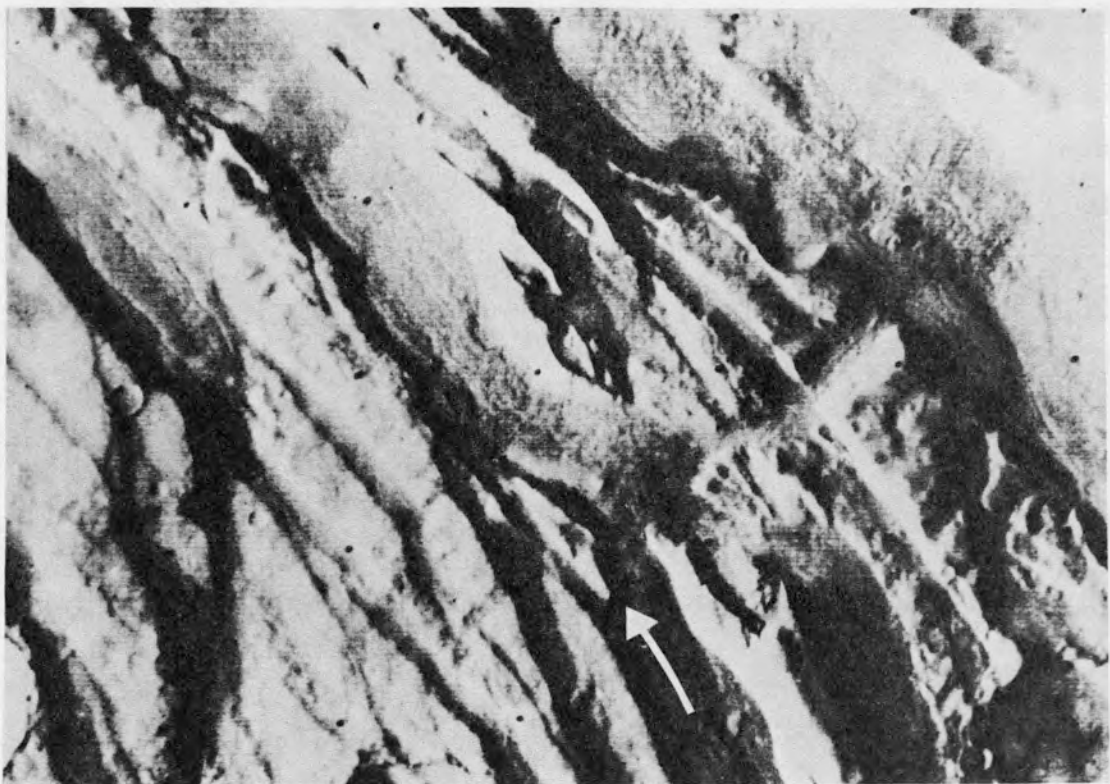
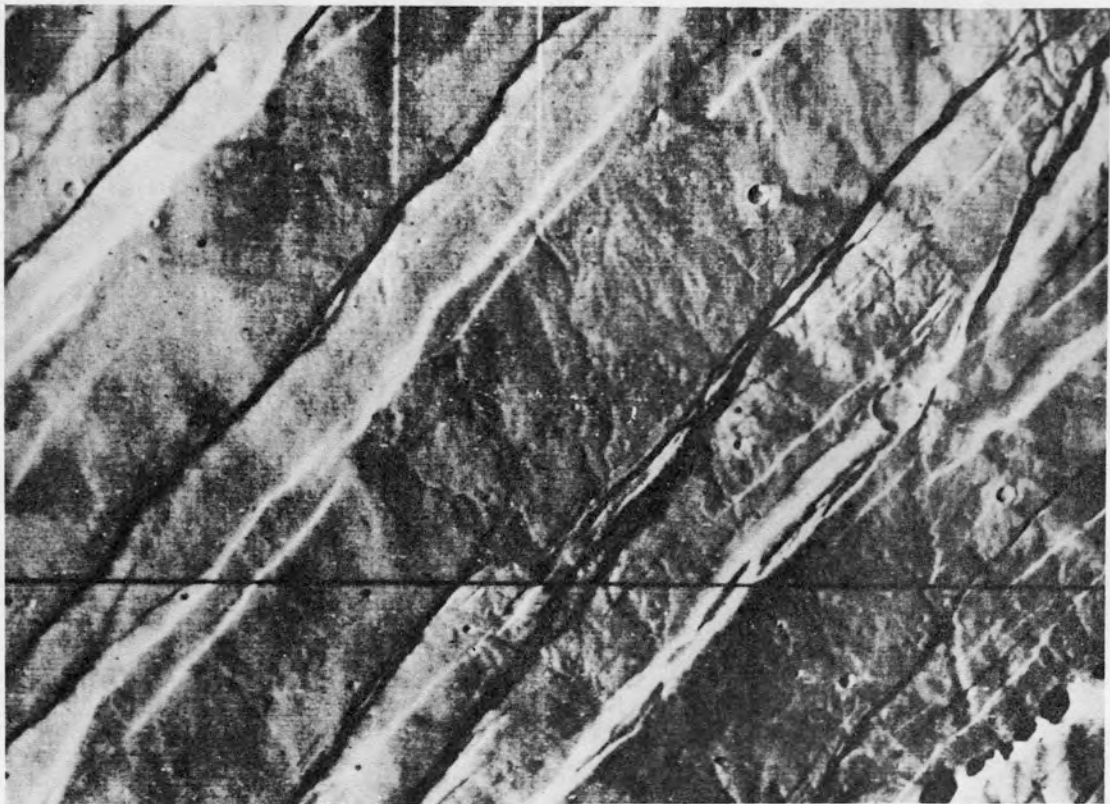
graben with the orientations and curvature observed.

Are these graben geometrically distinguishable from graben formed by another process? We are by no means finished with our efforts to answer this question, but preliminary results seem to indicate that individual graben may not be. The curvature of the entire complex, however, provides a clue if we have other evidence indicating that subsurface flow towards the concave side of the arc is reasonable. Curvature of graben sets on Mars and the moon can be due to inheritance from earlier structures with a near-circular plan shape, such as craters, basins, or volcanoes, so curvature alone, without independent evidence suggesting the possibility of flow, is not diagnostic.

Solutions to the key questions concerning the thickness of the brittle layer above the zone or layer of flow, and the amount of lateral extension implied by the graben visible on the surface require knowledge of the three-dimensional geometry of the graben. Only by combining field, experimental, and theoretical studies can we hope to unravel the three-dimensional geometry of structures on other planets.

Figure 48: Graben in the Tharsis region of Mars. Note ramp-like ends on those graben segments that terminate within this photograph. Graben walls are characterized by many benches with no indication of inward rotation, suggesting that the bounding faults are probably not vertical. NASA, Mariner 9 frame DAS 08443059. Dimensions of area shown approximately 50Km x 70Km.

Figure 49: Graben near the Tharsis ridge of Mars. Note slabs dropped into large graben across center of picture. These appear to be rotated outward, away from the axis of the graben, consistent with motion on faults inclined inward towards the graben floor (Figs. 17, 40 and 41). The slab that seems to illustrate this most clearly is indicated with an arrow. NASA, Mariner 9 frame DAS 08227039. Dimensions of area shown approximately 50Km x 70Km.



## REFERENCES

- Anderson, E.M., 1951, The dynamics of faulting and dyke formation with applications to Britain, Ed. 2: Edinburgh and London, Oliver and Boyd, 206p.
- Baars, D.L., 1962, Permian system of Colorado Plateau: Am. Assoc. Petroleum Geologists Bull., V. 46, p. 149-218.
- Baker, A.A., 1933, Geology and oil possibilities of the Moab district, Grand and San Juan Counties, Utah: U.S. Geol. Survey Bull. 841, 95p.
- \_\_\_\_\_, 1946, Geology of the Green River Desert-Cataract Canyon region, Emery, Wayne, and Garfield Counties, Utah: U.S. Geol. Survey Bull. 951, 122p.
- Baldwin, R.B., 1971, Rima Goclenius II: Jour. Geophysical Res., V. 74, p. 8459-8465.
- Griggs, D., and Handin, J., 1960, Observations on fracture and a hypothesis of earthquakes: Geol. Soc. America, Mem. 79, p. 347-364.
- Harrison, T.S., 1927, Colorado-Utah salt domes: Am. Assoc. Petroleum Geologists Bull., V. 11, p. 111-133.
- Hartmann, W.K., 1973, Martian cratering, 4, Mariner 9 initial analysis of cratering chronology: Jour. Geophysical Res., V. 78, p. 4096-4116.
- Hubbert, M.K., 1951, Mechanical basis for certain familiar geologic structures: Geol. Soc. America Bull., V. 62, p. 355-372.
- Hunt, C.B., 1969, Geologic history of the Colorado River: U.S. Geol. Survey, Prof. Paper 669-C, p. 59-130.
- Johnson, A.M., and Pollard, D.D., 1973, Mechanics of growth of some laccolithic intrusions in the Henry Mountains, Utah, I. Field observations, Gilbert's model, physical properties and flow of the magma: Tectonophysics, V. 18, p. 261-309.
- Lewis, R.Q., Sr., and Campbell, R.H., 1965, Geology and uranium deposits of Elk Ridge and vicinity, San Juan County, Utah: U.S. Geol. Survey, Prof. Paper 474-B, 69p.
- McGill, G.E., 1971, Attitude of fractures bounding straight and arcuate lunar rilles: Icarus, V. 14, p. 53-58.

- Meier, M.F., 1960, Mode of flow of Saskatchewan glacier, Alberta, Canada: U.S. Geol. Survey, Prof. Paper 351, 68p.
- Nye, J.F., 1951, The flow of glaciers and ice-sheets as a problem in plasticity: Proc. Roy. Soc. London, ser. A, V. 207, p. 554-572.
- \_\_\_\_\_, 1952, The mechanics of glacier flow: Jour. Glaciology, V. 2, p. 82-93.
- \_\_\_\_\_, 1957, The distribution of stress and velocity in glaciers and ice-sheets: Proc. Roy. Soc. London, ser. A, V. 239, p. 113-133.
- \_\_\_\_\_, 1965, The flow of a glacier in a channel of rectangular, elliptic or parabolic cross section: Jour. Glaciology, V. 5, p. 661-690.
- Phillips, R.J., Saunders, R.S., and Conel, J.E., 1973, Mars: crustal structure inferred from Bouguer gravity anomalies: Jour. Geophysical Res., V. 78, p. 4815-4820.
- Quaide, W., 1965, Rilles, ridges, and domes - clues to maria history: Icarus, V. 4, p. 374-389.
- Sagan, C., Toon, D.B., and Gierasch, P.J., 1973, Climatic change on Mars: Science, V. 181, p. 1045-1049.
- Sharp, R.P., Soderblom, L.A., Murray, B.C., and Cutts, J.A., 1971: The surface of Mars, 2, uncratered terrains: Jour. Geophysical Res., V. 76, p. 331-342.

